Lymphotoxin β Receptor: a Crucial Role in Innate and Adaptive Immune Responses against *Toxoplasma gondii*

Anne Tersteegen,[a,d] Ursula R. Sorg,[a] Richard Virgen-Slane,[b] Marcel Helle,[a] Patrick Petzsch,[c] Ildiko R. Dunay,[d] Karl Köhrer,[c] Daniel Degrandi,[a] Carl F. Ware,[b] Klaus Pfeffer[a]

[a]Institute of Medical Microbiology and Hospital Hygiene, Heinrich Heine University, Düsseldorf, Germany
[b]Laboratory of Molecular Immunology, Infectious and Inflammatory Diseases Center, Sanford Burnham Prebys Medical Discovery Institute, La Jolla, California, USA
[c]Biological and Medical Research Center (BMFZ), Heinrich Heine University, Düsseldorf, Germany
[d]Institute of Inflammation and Neurodegeneration, Otto-von-Guericke-University, Magdeburg, Germany

ABSTRACT The lymphotoxin β receptor (LTβR) plays an essential role in the initiation of immune responses to intracellular pathogens. In mice, the LTβR is crucial for surviving acute toxoplasmosis; however, until now, a functional analysis was largely incomplete. Here, we demonstrate that the LTβR is a key regulator required for the intricate balance of adaptive immune responses. *Toxoplasma gondii*-infected LTβR-deficient (LTβR$^{-/-}$) mice show globally altered interferon-γ (IFN-γ) regulation, reduced IFN-γ-controlled host effector molecule expression, impaired T cell functionality, and an absent anti-parasite-specific IgG response, resulting in a severe loss of immune control of the parasites. Reconstitution of LTβR$^{-/-}$ mice with toxoplasma immune serum significantly prolongs survival following *T. gondii* infection. Notably, analysis of RNA-seq data clearly indicates a specific effect of *T. gondii* infection on the B cell response and isotype switching. This study uncovers the decisive role of the LTβR in cytokine regulation and adaptive immune responses to control *T. gondii*.

KEYWORDS lymphotoxin, *Toxoplasma gondii*, host-pathogen interactions

The lymphotoxin β receptor (LTβR) is one of the core members of the tumor necrosis factor (TNF)/TNF receptor (TNFR) superfamily (1, 2). It has two cognate ligands, LTβ (LT$\alpha_1\beta_2$) and LIGHT (homologous to lymphotoxins, exhibits inducible expression, and competes with herpesvirus [HSV] glycoprotein D for herpesvirus entry mediator [HVEM], a receptor expressed by T lymphocytes) (3, 4). LTβR-mediated signaling is known to be essential for the organogenesis of secondary lymphoid tissues, the maintenance of their structure, and its role in mediating innate immune responses to many pathogens is also well documented (2, 5–7). LTβR-deficient (LTβR$^{-/-}$) mice lack lymph nodes (LNs) and Peyer's patches (PPs), show reduced numbers of natural killer (NK) cells and dendritic cells (DCs) as well as impaired immunoglobulin (Ig) affinity maturation (7, 8). In infection models, LTβR$^{-/-}$ mice show pronounced defects in their immune response against *Listeria monocytogenes*, *Mycobacterium tuberculosis* (5), cytomegalovirus (9), lymphocytic choriomeningitis virus (LCMV) (10), and Zika virus (11), as well as *Toxoplasma gondii* (*T. gondii*) (12). In spite of these extensive deficits, not much is known about the exact role of LTβR signaling for efficient generation of the immune response against pathogens.

T. gondii, the causative agent of toxoplasmosis, is an obligate intracellular parasite belonging to the Apicomplexa. It is able to invade most warm-blooded vertebrates, including humans (13, 14), and can infect all nucleated cells. While acute toxoplasmosis usually presents with only mild, flu-like symptoms in immunocompetent hosts, it sometimes manifests as lymphadenitis, hepatosplenomegaly, myocarditis, or pneumonia. In immunocompromised patients, toxoplasmosis can cause serious health

problems and, when primary infection occurs during pregnancy, severe congenital defects may occur (15–17).

The early immune response to *T. gondii* is characterized by recognition of *T. gondii*-associated molecules (i.e., profilin) by different cell types, such as DCs. These cells produce distinct cytokines in response to infection, such as interleukin-12 (IL-12) and TNF, thus activating and stimulating other cell types, including NK cells (18), T cells (19), innate lymphoid cells (ILCs) (20), and macrophages (21), which in turn, produce inflammatory cytokines such as IFN-γ.

IFN-γ signaling is essential for limiting *T. gondii* proliferation during the acute stage of toxoplasmosis and driving the parasite into the chronic stage, where it is contained by a functional immune response (22–25). IFN-γ-driven effector mechanisms include induction of cell-autonomous effector mechanisms (26, 27), such as depletion of tryptophan (28) and reactive nitrogen production (29), which suppress *T. gondii* replication and are essential for restricting parasite growth. IFN-γ also strongly induces murine guanylate-binding proteins (mGBPs), which play a major role in restricting parasite growth of *T. gondii* as well as other intracellular pathogens (30–33). Within an infected cell, *T. gondii* resides within a parasitophorous vacuole (PV) that effectively protects the parasite from lysosomal activity (34). mGBPs are recruited to the PV and are instrumental in destroying first the PV and then the parasites within (30, 31, 33, 35, 36).

Previous studies have shown that other core members of the TNF/TNFR superfamily, such as the ligands TNF and LTα, which signal via the TNFRI receptor, also play an important part in the immune response to *T. gondii* (25, 37, 38). However, there is only limited data published on the role of the LTβR; it has been demonstrated that signaling via the LTβR is essential for the upregulation of mGBPs after *T. gondii* infection as well as for overall survival (12). Glatman Zaretsky et al. have shown that LTβ signaling is important for maintaining intact splenic architecture and, indirectly, for efficient *T. gondii*-specific antibody production in *T. gondii* type II strains (Prugniaud) (39). Nevertheless, the pathophysiology responsible for the increased susceptibility of LTβR$^{-/-}$ mice to *T. gondii* infection is still elusive.

Here, we demonstrate that LTβR deficiency results in dramatically dysregulated IFN-γ responses, impaired expression of antiparasite effector molecules, limited T cell functionality, and an abrogated *T. gondii* specific IgG response. We show that by transfer of *T. gondii* immune serum, survival of LTβR$^{-/-}$ mice can be prolonged, demonstrating that the susceptibility of LTβR$^{-/-}$ mice to *T. gondii* infection is possibly due to a direct role of LTβR signaling in Ig class switch. These results lead to a new understanding of LTβR-mediated immunity and the pathophysiology of toxoplasmosis and will hopefully aid in developing much-needed new treatment and prevention options such as passive vaccination strategies for human toxoplasmosis.

RESULTS

LTβR deficiency leads to increased parasite burden in lung, spleen, and muscle. While wild-type C57BL/6 (WT) mice survive a *T. gondii* infection, LTβR$^{-/-}$ mice are highly susceptible to *T. gondii* infection and do not survive beyond day 14 postinfection (p.i.) (Fig. 1a). This high susceptibility is in accordance with our previous study (12). To characterize the cause of this susceptibility in LTβR$^{-/-}$ mice, we first assessed the parasite burden in *T. gondii*-infected WT and LTβR$^{-/-}$ animals during the acute phase of infection via quantitative realtime PCR (qRT-PCR) (Fig. 1b). In lung tissue, we found increasing amounts of *T. gondii* DNA up to day 10 p.i. in both cohorts, with significantly larger amounts in LTβR$^{-/-}$ than WT mice on day 10 p.i. In the spleen, *T. gondii* DNA amounts increased only moderately in WT mice through the course of infection (Fig. 1b). In contrast, LTβR$^{-/-}$ mice showed a significant increase of *T. gondii* DNA by day 10 p.i. and significantly increased amounts compared to WT mice on days 7 and 10 p.i. Interestingly, in both genotypes, reduced amounts of *T. gondii* DNA were detected on day 10 compared to day 7 p.i. Similar results were observed in muscle tissue (Fig. 1b). In WT mice, the parasite burden rose only moderately, while LTβR$^{-/-}$ mice showed a significant increase by day 10 p.i. as well as significantly larger amounts on days 7 and 10 p.i. To summarize, LTβR$^{-/-}$ mice showed increased parasite
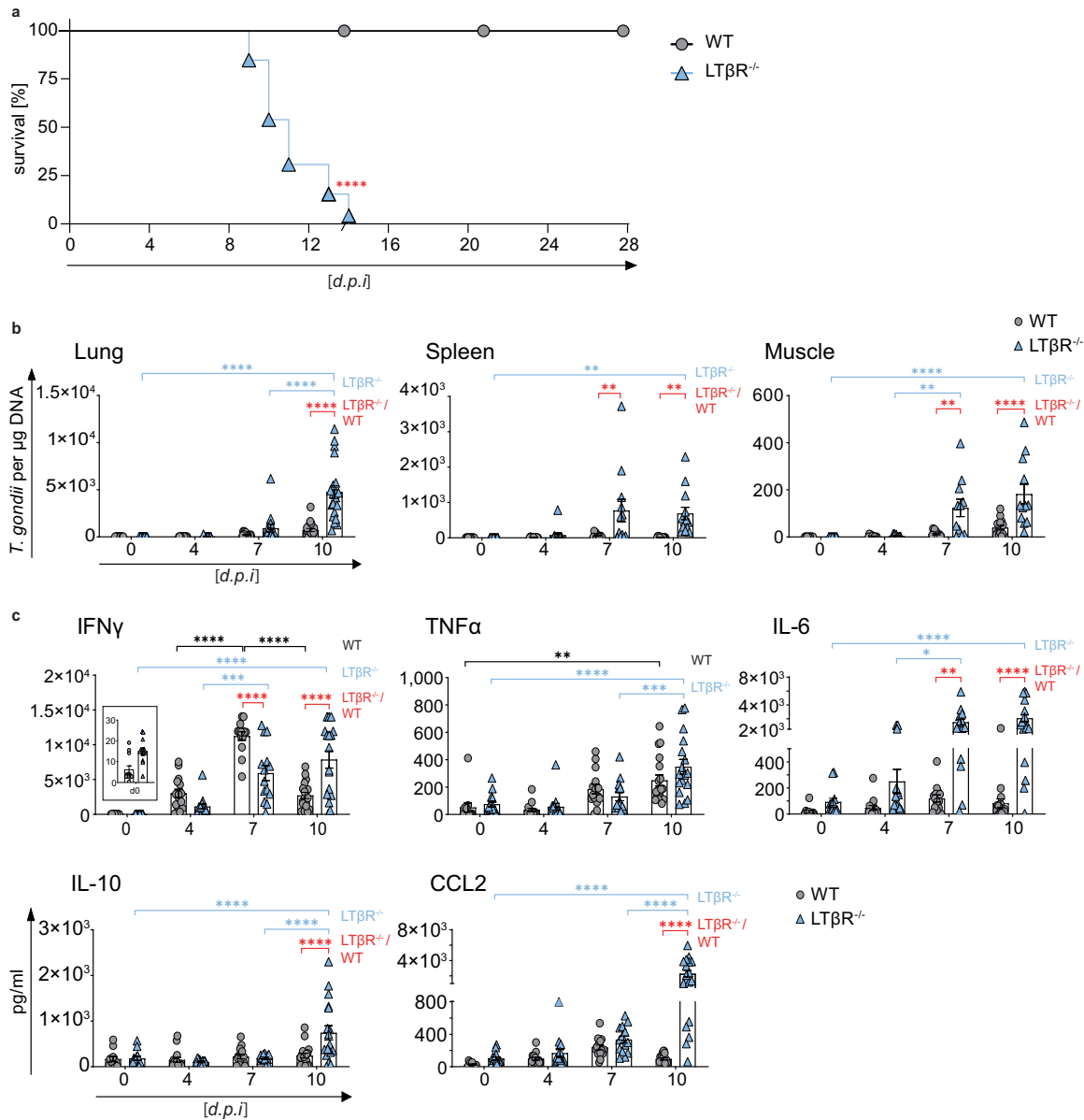
FIG 1 LTβR$^{-/-}$ mice show increased parasite load and dysregulated cytokine expression. (a) Survival of *T. gondii*-infected (ME49, 40 cysts, i.p.) WT ($n = 15$) and LTβR$^{-/-}$ ($n = 13$) mice. (b) qRT-PCR analysis of *T. gondii* DNA (assessing parasite load) in lung, spleen, and muscle tissue of uninfected (d0) and *T. gondii*-infected WT and LTβR$^{-/-}$ mice (d0 to d7, $n \geq 12$; d10, $n \geq 14$). (c) Expression of IFN-γ, TNF-α, IL-6, IL-10, and CCL2 in the serum of uninfected and *T. gondii*-infected WT and LTβR$^{-/-}$ mice (d0 to d7, $n \geq 12$; d10, $n = 18$) analyzed via bead-based immunoassay. The data shown represent at least three independent experiments; symbols represent individual animals, columns represent mean values, and error bars represent the ± SEM. A log rank (Mantel Cox) test was used for statistical analysis represented in panel a. Two-way ANOVA corrected for multiple comparison using Tukey's *post hoc* test was used for the statistical analysis represented in panels b and c. *, $P < 0.0332$; **, $P < 0.0021$; ***, $P < 0.0002$; ****, $P < 0.0001$.

burden compared to WT mice, pointing toward a failure of these animals to adequately control parasite proliferation in the acute phase of infection.

Dysregulated cytokines in the serum of LTβR$^{-/-}$ mice after infection with *T. gondii*. Since cytokines, especially IFN-γ and TNF-α, as signature molecules of a Th1 response play an important role in containing *T. gondii* expansion (16, 22, 40), we analyzed cytokine amounts in sera of infected mice (Fig. 1c). In both genotypes IFN-γ amounts increased slightly by day 4 p.i. In WT animals, IFN-γ amounts increased significantly by day 7 p.i. but were found to be markedly decreased again on day 10 p.i. While LTβR$^{-/-}$ mice also showed a significant increase of IFN-γ expression on day 7 p.i., amounts were

significantly lower than those of WT animals. Also, in LTβR$^{-/-}$ mice, IFN-γ expression levels were significantly higher on day 10 p.i. than those of WT animals. TNF-α expression increased significantly in WT as well as LTβR$^{-/-}$ animals by day 10 p.i. and did not differ significantly between the two genotypes, although amounts in LTβR$^{-/-}$ mice seemed to rise more steeply later in infection (day 7 versus day 10 p.i. for WT and LTβR$^{-/-}$ mice, respectively).

In WT animals, expression of IL-6, another proinflammatory cytokine (41), was slightly increased on day 4 and day 7 p.i. but was reduced again on day 10 p.i. (Fig. 1c). In contrast, in LTβR$^{-/-}$ mice, IL-6 amounts rose significantly during the course of infection and were significantly higher on days 7 and 10 p.i. than those of WT mice. Amounts of IL-10, known for its anti-inflammatory properties during infection (42), did not change significantly in WT animals during the course of infection (Fig. 1c). In contrast, amounts in LTβR$^{-/-}$ animals rose significantly on day 10 p.i. and were significantly higher than those of WT mice. The monocyte chemotactic factor (CCL2), a chemokine described to be induced by *T. gondii* (43), increased in WT as well as LTβR$^{-/-}$ mice on days 4 and 7 p.i. But while CCL2 in WT mice declined again by day 10 p.i., CCL2 further increased in LTβR$^{-/-}$ mice on day 10 p.i. and was significantly higher than in WT mice (Fig. 1c). Interestingly, LTβR$^{-/-}$ mice showed increased baseline amounts (day 0) for IFN-γ, TNF-α, IL-6, and CCL2 compared to WT mice, even though these differences were not significant.

Significantly different amounts were detected for IFN-β, IL-1α, IL-23, and IL-27 only on day 4 p.i. (see Fig. S1 in the supplemental material). LTβR$^{-/-}$ animals showed increased baseline amounts (day 0) for IFN-β, IL-1α, IL-1β, IL-17A, IL-23, IL-27, and IL-12p70, which were, however, significant only in the case of IL-1β. No differences in IL-12p70 levels were detected for the two genotypes (Fig. S1).

To summarize, uninfected LTβR$^{-/-}$ mice show different baseline amounts of proinflammatory cytokines, suggesting a subtle activation of the immune system. Furthermore, in these animals, the coordinated immune defense during *T. gondii* infection is dysregulated.

Markedly altered transcriptome in the lungs of LTβR$^{-/-}$ mice after *T. gondii* infection. The lungs are one of the target organs of *T. gondii* tachyzoite dissemination (12, 44). In line with that observation, we detected large amounts of *T. gondii* DNA in lung tissue of LTβR$^{-/-}$ compared to WT mice on day 4 p.i. (Fig. 1b). To determine whether WT and LTβR$^{-/-}$ mice show differences in global gene expression patterns in the lungs, we analyzed lung tissue via transcriptome sequencing (RNA-seq) on day 7 p.i. Interestingly, gene set enrichment analysis (GSEA) of these data showed a significant upregulation of Gene Ontology (GO) (biological process) molecular signatures for "response to type I interferons, response to interferon gamma, and interferon gamma mediated signaling pathway" in *T. gondii*-infected WT compared to LTβR$^{-/-}$ mice on day 7 p.i. (Fig. S2). The data depicted by a volcano plot (Fig. 2a) clearly show a significant upregulation of IFN-γ-regulated genes in *T. gondii*-infected WT mice compared to LTβR$^{-/-}$ mice (day 7 p.i.); for instance, transcripts for mGBPs (mGBP2b/1, 2, 6, 7, and 10), transcripts for effector molecules (IDO1, Gzmk), transcripts for chemokines and chemokine receptors responsible for recruitment of immune cells (CCL2, CCL4, CCL7, CXCL9, CXCL10, CCR1), transcripts for proteins involved in IFN-γ signaling (IRF1, STAT1), transcripts induced by IFN-γ (TGTP1, PIM1), and other transcripts known to be involved in immune responses (CD274, IL12Rb1, Ly6i, Ly6c2, MMP8, RNF19b) were found to be highly expressed in infected WT but not in LTβR$^{-/-}$ lungs on day 7 p.i. This suggests that LTβR$^{-/-}$ mice fail to adequately upregulate (IFN-γ-dependent) immune responses in the lung.

LTβR deficiency leads to dysregulation of cytokine expression in the lung. To add additional kinetic data RNA-seq data (Fig. 2a) and cytokine levels in serum (Fig. 1c; Fig. S1), we determined mRNA expression levels of cytokines in the lungs of infected WT and LTβR$^{-/-}$ mice at several time points after infection (Fig. 2b and c). Baseline expression levels of IFN-γ were higher in LTβR$^{-/-}$ animals; thus, while levels rose on day 4 p.i. in both genotypes, this increase was only significant in WT mice (Fig. 2b). While IFN-γ mRNA levels were markedly decreased in WT mice by day 10 p.i., they were still markedly but not significantly elevated in LTβR$^{-/-}$ mice (Fig. 2b). Baseline expression of TNF-α was
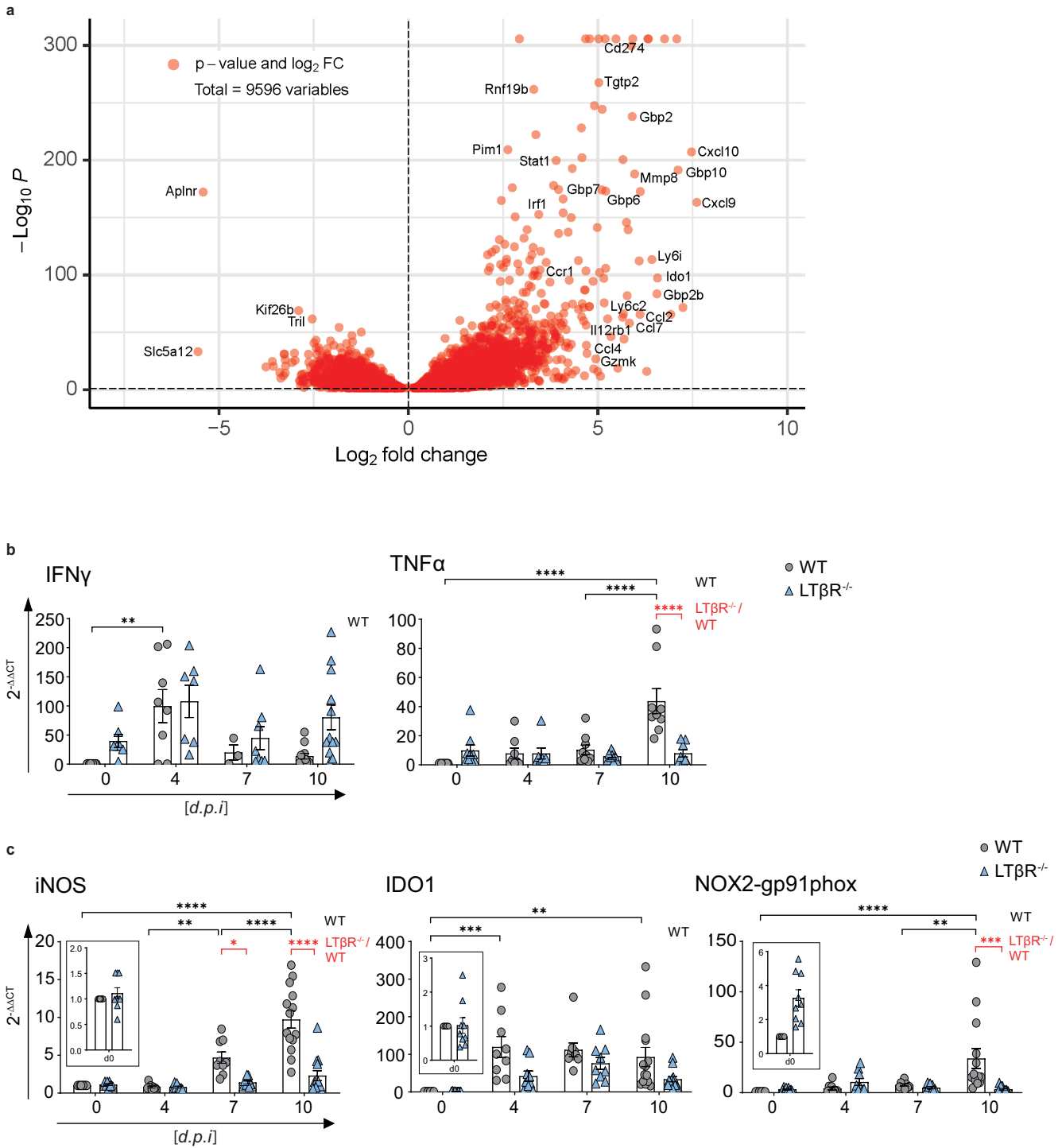
FIG 2 Lungs of LTβR$^{-/-}$ mice show an altered transcriptome after *T. gondii* infection. (a) Volcano plot showing RNA-seq data of lung tissue of infected WT mice correlated with infected LTβR$^{-/-}$ mice (d7 p.i.; $n = 3$/group). The dashed horizontal black line represents an adjusted P value of 0.1 (Wald test). (b and c) qRT-PCR analysis of (b) cytokines (IFN-γ and TNF-α) and (c) host effector molecules (iNOS, IDO1, NOX2-gp91phox) in lung tissue from uninfected (d0) and *T. gondii*-infected (ME49, 40 cysts, i.p.) WT and LTβR$^{-/-}$ mice (d0 to 7, $n \geq 12$; d10, $n \geq 14$; exception: IFN-γ, $n \geq 3$, d0 to 10 p.i.). Data shown in panels b and c represent four independent experiments; symbols represent individual animals, columns represent mean values, and error bars represent the ± SEM. Two-way ANOVA corrected for multiple comparison using Tukey's *post hoc* test was used for the statistical analysis. *, $P < 0.0332$; **, $P < 0.0021$; ***, $P < 0.0002$; ****, $P < 0.0001$.

increased in LTβR$^{-/-}$ mice but did not change significantly during the course of infection. WT mice showed a significant increase in TNF-α expression on day 10 p.i. (Fig. 2b), indicating a significant difference in the cytokine response between the two genotypes on day 10 p.i. Baseline expression levels of LTβ were significantly increased in LTβR$^{-/-}$ mice, which could

be due to a lack of negative feedback or compensatory mechanisms. However, while levels tended to be higher in LTβR$^{-/-}$ animals throughout the infection, there were no significant differences in LTβ expression between the two genotypes (Fig. S3). IL-4 expression was significantly increased in WT animals on day 10 p.i. compared to baseline expression. In LTβR$^{-/-}$ mice, IL-4 expression was comparable to that of WT mice but not significantly increased on day 10 p.i. compared to baseline expression (Fig. S3). These data confirm that LTβR$^{-/-}$ mice show a dysregulated immune homeostasis not only in serum (Fig. 1c; Fig. S1) but also in lung tissue after *T. gondii* infection.

LTβR deficiency leads to impaired IFN-γ-regulated effector molecule expression in the lung. IFN-γ-regulated effector molecules are pivotal in *T. gondii* elimination (31, 33, 45), having important immune response functions. In particular, the roles of effector molecules, such as iNOS, IDO, and NOX2-gp91phox (46–48), are well documented. Since RNA-seq data (Fig. 2a) showed high expression of effector molecules in infected WT, but not LTβR$^{-/-}$ (31) mice we assessed the expression of major effector molecules in lungs by qRT-PCR next (Fig. 2c). In contrast to WT mice, LTβR$^{-/-}$ mice failed to upregulate iNOS expression postinfection, leading to significant differences between the two genotypes on days 7 and 10 p.i. WT mice showed significant upregulation of IDO1 expression on day 4 p.i. and had significantly increased IDO1 expression levels on day 10 p.i., whereas LTβR$^{-/-}$ mice showed only a minor increase of IDO1 expression, and this difference was not significant compared to baseline expression. NOX2-gp91phox presented a similar picture—significantly increased NOX2-gp91phox expression in WT animals on day 10 p.i. compared to baseline expression as well as compared to LTβR$^{-/-}$ mice and a complete failure of upregulation of NOX2-gp91phox in the absence of LTβR. The failure to adequately upregulate IFN-γ-regulated effector molecules involved in cell intrinsic defense mechanisms essential for suppressing *T. gondii* replication most likely contributes to the increased parasite burden observed in LTβR$^{-/-}$ animals.

LTβR deficiency leads to impaired IFN-γ-induced mGBP expression and IFN-γ signaling in the lung. Another important group of genes upregulated in an IFN-γ-dependent manner after *T. gondii* infection are mGBPs (30). These GTPases have been shown to be essentially involved in *T. gondii* elimination (30–33). A heat map for mGBP expression data (Fig. 3a) was generated from the RNA-seq data, illustrating an overall slight increase in baseline mGBP expression in uninfected (day 0) LTβR$^{-/-}$ mice compared to WT mice but an overall lower mGBP expression in LTβR$^{-/-}$ compared to WT mice on day 7 p.i. These results were confirmed by qRT-PCR analysis of mGBP mRNA expression; for all mGBPs analyzed (mGBP1, 2, 3, 5, 6/10, 7, 8, and 9), we observed a significant increase in mGBP expression ($P < 0.0001$ in all cases) in WT animals by day 10 p.i. (Fig. 3b). In contrast, in LTβR$^{-/-}$ mice, a significant rise on day 10 p.i. compared to baseline expression was only observed for mGBP2, mGBP3, and mGBP7. Also, expression levels of all mGBPs were significantly higher in WT mice than in to LTβR$^{-/-}$ mice on day 10 p.i., with the exception of mGBP6/10, where expression levels were only slightly increased in WT mice. The failure to adequately upregulate expression of mGBPs early after *T. gondii* infection was further confirmed by immunoblot analysis, where upregulation of mGBP2 and mGBP7 protein expression was already detectable on day 4 p.i. in WT mice but not in LTβR$^{-/-}$ mice (Fig. 3c; Fig. S4). This defect in upregulation of mGBP expression after *T. gondii* expression likely has a major effect on the ability of LTβR$^{-/-}$ mice to contain parasite replication, as mGBPs are essential for an effective immune response against this parasite (31–33).

Since protein expression of IFN-γ-induced mGBPs was affected in lungs of LTβR$^{-/-}$ mice in *T. gondii* infection, we further analyzed protein expression of prototype genes directly involved in IFN-γR signaling (Fig. 3c; Fig. S4). Protein expression levels of STAT1, pSTAT1, IRF-1, and pSTAT3 increased in WT mice during the course of infection. In contrast, LTβR$^{-/-}$ animals showed a marked delay in the upregulation of these proteins. In WT animals, JAK1 and STAT3 expression increased until day 7 p.i. but decreased again on day 10 p.i. In uninfected LTβR$^{-/-}$ mice, expression of these proteins was higher than in uninfected WT mice but did not increase early in infection. This also provides evidence for an altered IFN-γ/IFN-γR signaling axis during *T. gondii* infection.
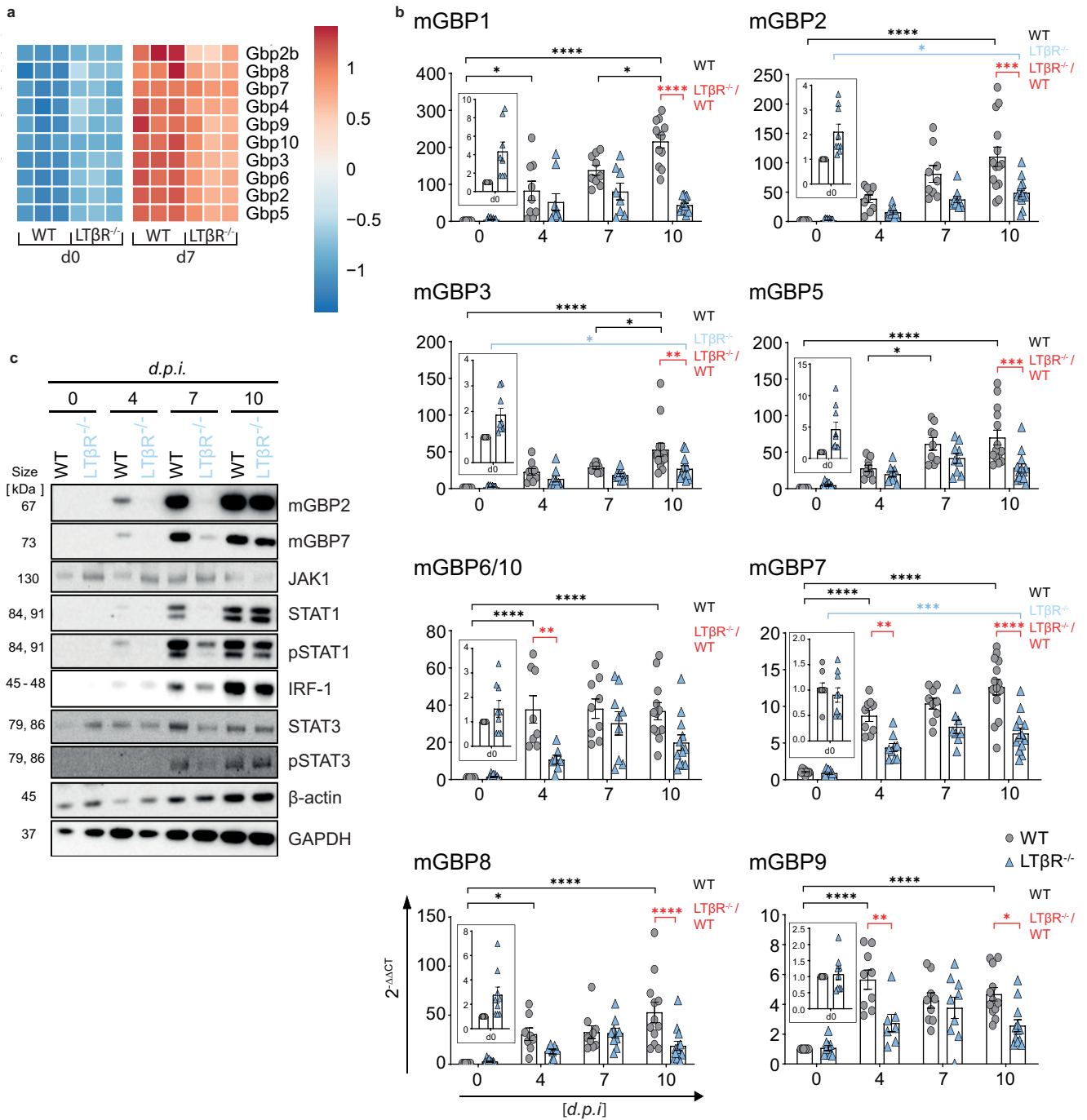
FIG 3 LTβR deficiency dysregulates IFN-γ signaling in the lung. (a) Heat map of differentially expressed murine guanylate-binding proteins (mGBPs) based on RNA-seq analysis (Wald test and adjusted *P* value of 0.1) of lung tissue from uninfected (d0) and *T. gondii*-infected (ME49, 40 cysts i.p., d7 p.i.) WT and LTβR$^{-/-}$ mice ($n = 3$). (b) qRT-PCR of mGBPs in lung tissue from uninfected and *T. gondii*-infected WT and LTβR$^{-/-}$ mice (d0 to 7, $n \geq 12$; d10, $n \geq 14$). The data shown represent four independent experiments; symbols represent individual animals, columns represent mean values, and error bars represent the ± SEM. (c) Immunoblot analysis of proteins involved in or induced via the IFN-γ signaling pathway in lung tissue from uninfected and *T. gondii*-infected WT and LTβR$^{-/-}$ mice. Two-way ANOVA corrected for multiple comparison using Tukey's *post hoc* test was used for the statistical analysis represented in panel b. *, $P < 0.0332$; **, $P < 0.0021$; ***, $P < 0.0002$; ****, $P < 0.0001$. The data shown in panel c are representative of three independent experiments.

To summarize, mRNA and protein expression data from the lungs indicate that uninfected LTβR$^{-/-}$ animals show an activated immune status compared to WT animals but fail to adequately upregulate IFN-γ-dependent immune effector responses after *T. gondii* infection, possibly explaining the increased parasite burden and the subsequently increased infection susceptibility of LTβR$^{-/-}$ mice.
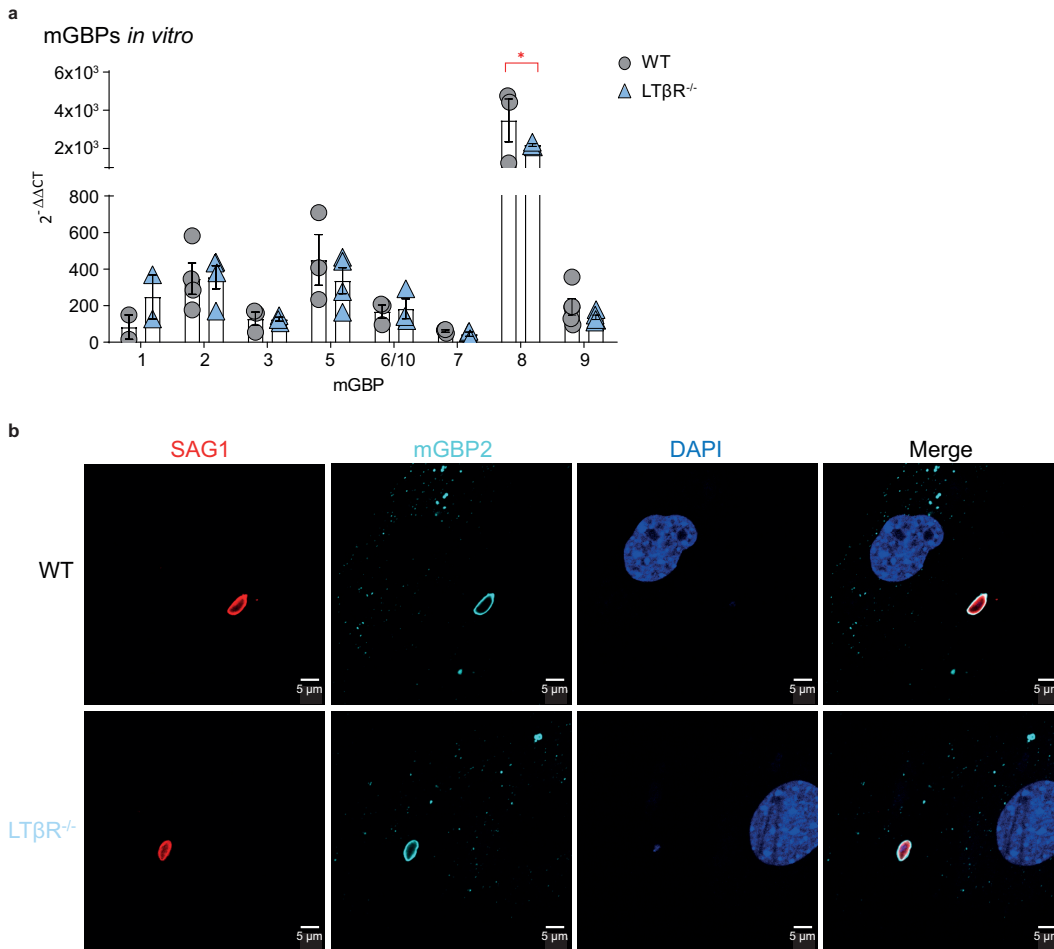
a

mGBPs *in vitro*

b

FIG 4 mGBP upregulation and recruitment. (a) qRT-PCR analysis of mGBP mRNA expression of uninfected WT and LTβR$^{-/-}$ MEFs stimulated with IFN-γ (7.5 ng/ml) for 8 h (all $n = 3$, except for mGBP1, where $n = 2$). Each symbol represents an individual technical replicate; columns represent mean values, and error bars represent the $\pm$ SEM. two-way ANOVA corrected for multiple comparisons by the Sidak *post hoc* test was used for statistical analysis. *, $P < 0.00332$. (b) Representative immunofluorescence analysis of *T. gondii* tachyzoite-infected (multiplicity of infection [MOI], 1:40) WT and LTβR$^{-/-}$ MEFs. Cells were prestimulated with IFN-γ (7.5 ng/ml) for 16 h before being infected with *T. gondii* tachyzoites for 2 h. *T. gondii* surface antigen SAG1 was visualized using a Cy3-conjugated secondary antibody, and mGBP2 was visualized using an mGBP2 antiserum (30) followed by an Alexa Fluor 633-conjugated secondary antibody for detection of mGBP2 recruitment toward the *T. gondii* PV. Cell nuclei were stained using DAPI (4′,6-diamidino-2-phenylindole). The data shown in panels a and b represent at least two independent experiments.

mGBP upregulation and recruitment to the PV after IFN-γ stimulation *in vitro*.
Since upregulation of mGBP expression was impaired in LTβR$^{-/-}$ mice after *T. gondii* infection (Fig. 3), we asked whether IFN-γ-dependent upregulation of mGBP expression was directly dependent on LTβR signaling (Fig. 4). We therefore analyzed whether LTβR$^{-/-}$ mouse embryonic fibroblasts (MEFs) were able to upregulate mGBPs after IFN-γ stimulation and whether mGBPs could recruit to the PV in infected, IFN-γ-pretreated LTβR$^{-/-}$ MEFs. After preincubation with IFN-γ *in vitro*, *T. gondii*-infected LTβR$^{-/-}$ and WT MEFs showed comparable upregulation of all tested mGBPs (mGBP1, 2, 3, 5, 6/10, 7, and 9), with the exception of mGBP8, where WT mice showed increased mRNA expression (Fig. 4a). Also, after preincubation with IFN-γ, mGBP2 was recruited to the PV of *T. gondii* in LTβR$^{-/-}$ MEFs (Fig. 4b). These results demonstrate that expression of mGBPs can be successfully induced in LTβR$^{-/-}$ MEFs in the presence of exogenous IFN-γ and that the lack of LTβR signaling appears not to interfere with the ability of mGBP2 to recruit to the PV in LTβR$^{-/-}$ MEFs. This suggests that the absence of LTβR signals do not impact IFN-γR signaling required for mGBP function.

Differences in spleen size and weight in LTβR$^{-/-}$ mice. Since LTβR$^{-/-}$ mice lack lymph nodes (7), the spleen is the primary organ where the immune response against *T. gondii* is primed. It has been described that during the acute phase of *T. gondii* infection, the splenic architecture is disrupted transiently (39). When we compared spleens of WT versus LTβR$^{-/-}$ mice, spleens of the latter were markedly larger (Fig. S5a) in uninfected (day 0) healthy animals. While spleens of both genotypes significantly increased in weight during the course of *T. gondii* infection, spleen weights of WT mice were significantly higher than those of LTβR$^{-/-}$ mice on day 10 p.i. (Fig. S5b). This increase of spleen weight in WT mice was not due to increased cellularity, as splenocyte counts were consistently higher in LTβR$^{-/-}$ spleens before as well as on days 4 and 7 p.i. (Fig. S5c). By day 10 p.i., cell numbers in the spleens of both genotypes were comparable, mostly due to a significant drop of splenocyte numbers in LTβR$^{-/-}$ mice. This also indicates that the initial immune response in spleens of LTβR$^{-/-}$ mice is disturbed.

No apparent difference in T cell subpopulations in spleens of LTβR$^{-/-}$ mice. Accordingly, we analyzed the composition of the splenocytes using flow cytometry (Fig. 5). Since T cells are essential to control *T. gondii* infection (49, 50), we analyzed T cell subpopulations in LTβR$^{-/-}$ spleens (Fig. 5a). Analysis of absolute numbers of CD3$^+$, CD4$^+$, CD8$^+$, activated (CD3$^+$CD25$^+$) T cells, and *T. gondii*-specific (pentamer$^+$) CD8$^+$ T cells (Fig. 5a) revealed almost no significant differences between WT and LTβR$^{-/-}$ mice either before or during infection. The only exception was CD4$^+$ T cells on day 4 p.i., where WT and LTβR$^{-/-}$ mice showed a moderate decrease and increase, respectively. In both genotypes, the numbers of activated CD3$^+$CD25$^+$ T cells were significantly increased on day 7 p.i., but LTβR$^{-/-}$ mice showed similar numbers of total T cells. In addition, LTβR$^{-/-}$ mice showed a comparable rise of activated CD3$^+$CD25$^+$ T cells on day 7 p.i. and a comparable expansion of *T. gondii*-specific (pentamer$^+$) CD8$^+$ T cells on day 10 p.i. (Fig. 5a).

Baseline numbers of CD19$^+$ B cells were somewhat higher in LTβR$^{-/-}$ mice and significantly increased on day 4 p.i., but while numbers of CD19$^+$ B cells dropped significantly in both genotypes on day 10 p.i., they were still significantly higher in LTβR$^{-/-}$ mice (Fig. 5b).

Since LTβR$^{-/-}$ mice are known to have fewer NK cells and NKT cells (8, 51, 52), it was not surprising to observe that absolute NK1.1$^+$ cells were significantly higher in WT than in LTβR$^{-/-}$ mice before infection and on days 4 and 7 p.i. (Fig. 5b). On day 10 p.i., NK1.1$^+$ cell numbers of both genotypes were similar, due to the drop of NK1.1$^+$ cells in spleens of WT mice during the course of infection. Similarly, the absolute numbers of NK1.1$^+$CD3$^+$ NKT cells in WT mice declined during the course of infection but were higher than those of LTβR$^{-/-}$ mice before infection and on days 4 and 7 p.i., which is in accordance with published data (51). Unbiased analysis of the cytometry data set using t-distributed stochastic neighbor embedding (tSNE) (Fig. 5c) confirmed these data, notably the absence of NK1.1$^+$ cells in uninfected LTβR$^{-/-}$ mice (1.46% and 0.04%, respectively) and the marked drop in absolute CD19$^+$ B cell numbers in WT mice by day 10 p.i. which was absent in LTβR$^{-/-}$ animals (59.03% to 2,26% versus 71.07% to 35.39%, respectively; Fig. 5c). This demonstrates that the deficiency of the LTβR does not impact T cell numbers after *T. gondii* infection, especially the expansion of parasite-specific T cells, while it does seem to influence B cell numbers during the acute phase of *T. gondii* infection.

In conclusion, LTβR$^{-/-}$ compared to WT mice do not show a significant difference in overall and antigen-specific T cell numbers either before or after *T. gondii* infection, but B cell, NK1.1$^+$, and NKT cell numbers appear to be significantly affected by the absence of LTβR before and during infection.

Impaired T cell effector function in the spleen in the absence of the LTβR. Even though LTβR$^{-/-}$ mice are highly susceptible to *T. gondii* infection, we detected comparable CD8$^+$ and *T. gondii*-specific CD8$^+$ T cell numbers in the spleen (Fig. 5a). We therefore decided to determine whether these T cells were fully differentiated and functional with regard to their ability to produce IFN-γ, contained cytotoxic granules (GzmB$^+$ and perforin$^+$),
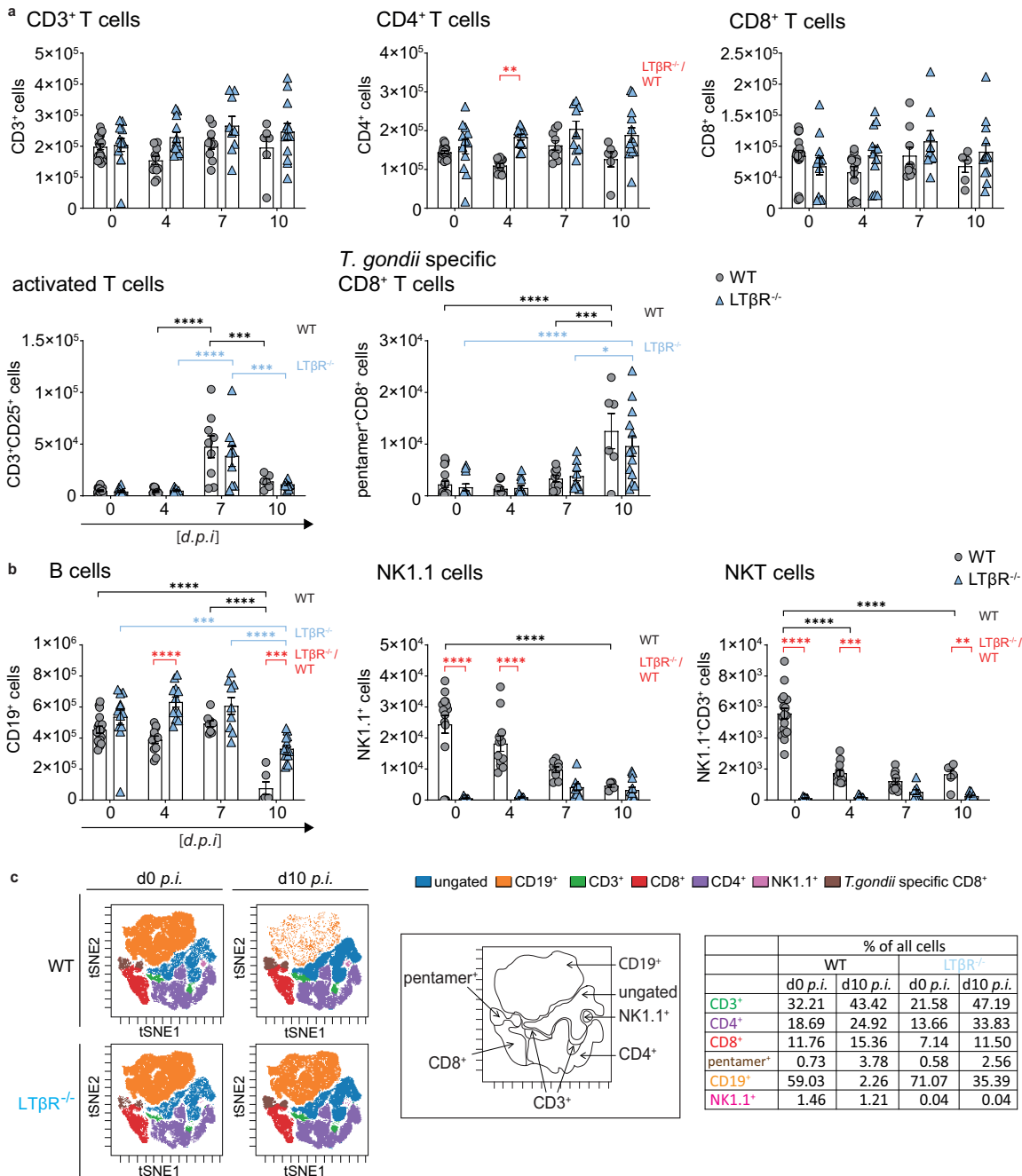
FIG 5 Dysregulated immune cell numbers in LTβR$^{-/-}$ mice. (a) Absolute cell numbers of CD3$^+$, CD4$^+$, CD8$^+$, CD25$^+$CD3$^+$, and pentamer$^+$CD8$^+$ T cells. (b) CD19$^+$, NK1.1$^+$, and NK1.1$^+$CD3$^+$ cells in spleens of uninfected (d0) and *T. gondii*-infected (ME49, 40 cysts, i.p.) WT and LTβR$^{-/-}$ mice (d0 to d7 p.i., $n = 12$; d10 p.i., $n \geq 6$) determined via flow cytometry. (c) Representative tSNE plots from splenocytes of uninfected and *T. gondii*-infected (d10 p.i.) WT and LTβR$^{-/-}$ mice. Clustered populations were identified using the indicated markers. The data shown represent at least three independent experiments; symbols represent individual animals, columns represent mean values, and error bars represent the $\pm$ SEM. Two-way ANOVA corrected for multiple comparison using Tukey's *post hoc* test was used for the statistical analysis represented in panels a and b. *, $P < 0.0332$; **, $P < 0.0021$; ***, $P < 0.0002$; ****, $P < 0.0001$.

and were able to degranulate (CD107a$^+$ cells) upon stimulation. In order to address this question, splenocytes of infected WT and LTβR$^{-/-}$ mice (day 7 and 10 p.i.) were prepared and were restimulated *ex vivo* with toxoplasma lysate antigen (TLA) before flow cytometry analysis (Fig. 6).

After *ex vivo* TLA restimulation, LTβR$^{-/-}$ T cells compared to WT T cells showed a significantly reduced frequency of CD4$^+$ IFN-γ-producing T cells in splenocytes from
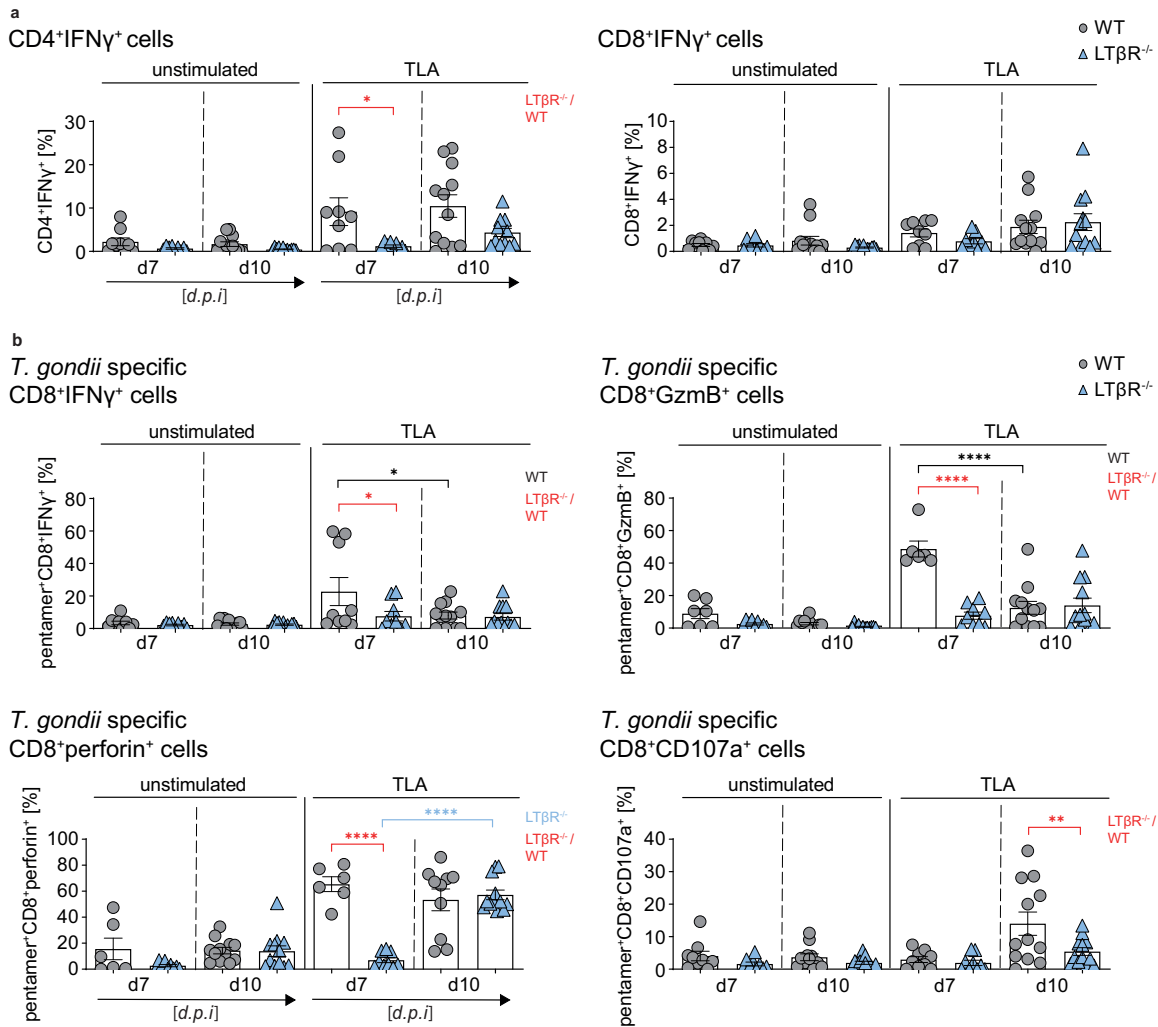
FIG 6 LTβR deficiency impairs T cell effector function in the spleen. (a and b) Intracellular staining of (a) CD4$^+$IFN-γ$^+$ and CD8$^+$IFN-γ$^+$ T cells (%) and (b) cytotoxic granule (GzmB$^+$ or perforin$^+$) containing and degranulating (CD107a$^+$) pentamer$^+$CD8$^+$ T cells of unstimulated and toxoplasma lysate antigen (TLA) *ex vivo* restimulated splenocytes from *T. gondii*-infected (d7 and 10 p.i.) WT and LTβR$^{-/-}$ mice (d7, $n \geq 6$; d10, $n \geq 10$). Representative data of at least two independent experiments; symbols represent individual animals, columns represent mean values, and error bars represent the ± SEM. Two-way ANOVA corrected for multiple comparison using Tukey's *post hoc* test was used for statistical analysis. *, $P < 0.0332$; **, $P < 0.0021$; ****, $P < 0.0001$.

day 7 p.i. and a reduced percentage in splenocytes at day 10 p.i. Similar frequencies for CD8$^+$ IFN-γ-producing T cells could be detected in restimulated splenocytes for both genotypes on both days (Fig. 6a). There were no significant differences between the two genotypes for granzyme B-containing CD8$^+$ cells in restimulated cells from either day 7 or day 10 p.i. (Fig. S6a). For CD8$^+$perforin$^+$ cells, WT mice showed higher frequencies in day 10 restimulated cells, but LTβR$^{-/-}$ mice showed a delayed but significant increase from day 7 to day 10, resulting in frequencies similar to those of WT mice for day 10 p.i. (Fig. S6a). In contrast, CD8$^+$107a$^+$ T cell frequencies in WT spleens increased significantly in restimulated cells from day 10 p.i. and were significantly higher than those of LTβR$^{-/-}$ spleens (Fig. S6a). When we directly analyzed IFN-γ$^+$GzmB$^+$ and IFN-γ$^+$perforin$^+$ cells, we found a significantly higher frequency in restimulated splenocytes of WT mice at day 7 p.i. than those of LTβR$^{-/-}$ mice (Fig. S6b).

For *T. gondii*-specific (pentamer$^+$) CD8$^+$ T cells (Fig. 6b), we found a significantly higher frequency of pentamer$^+$CD8$^+$ IFN-γ-producing T cells in restimulated splenocytes from WT mice on day 7 p.i. compared to LTβR$^{-/-}$ mice but not in restimulated splenocytes from day 10 p.i. Interestingly, *T. gondii*-specific CD8$^+$GzmB$^+$ T cells showed

a similar picture—a significantly increased frequency in restimulated splenocytes from WT mice on day 7 p.i. compared to LTβR$^{-/-}$ mice and no difference of these cells in splenocytes from day 10 p.i. In WT compared to LTβR$^{-/-}$ spleens, *T. gondii*-specific CD8$^+$perforin$^+$ T cells were also significantly higher in restimulated WT splenocytes at day 7 p.i. However, here, LTβR mice showed a significantly increased frequency of CD8$^+$perforin$^+$ T cells in restimulated splenocytes from day 10 compared to day 7 p.i., resulting in similar frequencies for WT and LTβR$^{-/-}$ CD8$^+$perforin$^+$ T cells at day 10 p.i. Finally, the percentage of *T. gondii*-specific CD8$^+$CD107a$^+$ T cells was similar for both genotypes in restimulated splenocytes at day 7 p.i. but significantly increased for WT mice in restimulated splenocytes from day 10 p.i., whereas only few CD8$^+$ LTβR$^{-/-}$ T cells degranulated. To summarize, importantly, parasite-specific granzyme B granule containing (pentamer$^+$CD8$^+$GzmB$^+$) as well as degranulating (pentamer$^+$CD8$^+$CD107a$^+$) T cells do not appear to be detectable in LTβR$^{-/-}$ mice after *T. gondii* infection, whereas the increase of parasite-specific perforin granule-containing (pentamer$^+$CD8$^+$perforin$^+$) T cells seems to be delayed in LTβR$^{-/-}$ compared to WT mice. These results demonstrate that while the T cell compartment does not seem to be affected in regard to cell numbers, LTβR$^{-/-}$ mice show a clear functional defect in the parasite-specific CD8$^+$ T cell compartment as well as clearly decreased IFN-γ-producing CD4$^+$ T cells after infection.

LTβR deficiency abrogates *T. gondii*-specific isotype class switching. RNA-seq data of lung tissue from uninfected (day 0) and *T. gondii*-infected (day 7 p.i.) WT and LTβR$^{-/-}$ animals were further analyzed to elucidate the interaction between *T. gondii* and host immune responses. The data were filtered for differentially expressed genes, and hierarchical clustering was performed and illustrated as a sample dendrogram with a trait heat map (Fig. S7a) for identification of possible outliers. All tested samples showed adequate clustering and could, accordingly, be grouped into uninfected and infected WT and LTβR$^{-/-}$ mice. Next, gene expression data were condensed into 10 module eigengenes (ME0 to ME9; Fig. S7b) and used to generate a host-pathogen network prediction model (Fig. 7a) displaying the relationship between modules (ME) and experimental conditions. This model captures the influence of *T. gondii* infection ("Infection" in the figure), the LTβR$^{-/-}$ genotype ("Genotype"), and total *T. gondii* genes ("X") on host gene modules (ME0 to ME9) detected in each sample. Upon closer inspection, this model shows that LTβR expression (contained in ME6) is suppressed by the LTβR$^{-/-}$ genotype, which fits our experimental conditions. This model predicts that in WT mice, high expression of genes contained in ME6 suppresses genes contained in ME4 (top GO term "B cell receptor signaling pathway") while enhancing gene expression in ME3 (top GO term "lymphocyte differentiation"). This implies that the loss of the LTβR slightly increases ME4 levels (Fig. S7c; top GO term "B cell receptor signaling pathway"; Fig. 7a) containing genes for "immunoglobulin production" and "humoral immune response mediated by circulating immunoglobulin" during *T. gondii* infection. Furthermore, the network predicts that in LTβR$^{-/-}$ mice, *T. gondii* infection reduces ME3 levels (Fig. S7d; top GO term "lymphocyte differentiation"; Fig. 7a) containing genes for "B cell activation" and "isotype switching." In addition, GSEA generated from RNA-seq data also showed significant upregulation of these pathways, indicating a disturbed B cell response (Fig. S2).

Due to this highly surprising prediction, as well as the different B cell numbers of WT and LTβR$^{-/-}$ mice in the spleen on day 10 p.i. (Fig. 5a and c), we then asked whether an altered B cell-mediated humoral immune response could be directly involved in the high mortality of LTβR$^{-/-}$ mice after *T. gondii* infection. The presence of immunoglobulin M (IgM) and IgG antibodies specific for *T. gondii* antigens was determined during the acute phase of infection (days 4, 7, and 10 p.i.) using line blots coated with specific recombinant *T. gondii* tachyzoite and bradyzoite antigens (ROP1c, GRA7, GRA8, p30, and MAG1). LTβR$^{-/-}$ mice compared to WT mice showed a delayed and reduced *T. gondii*-specific IgM and, surprisingly, an abrogated *T. gondii*-specific IgG antibody response in the serum during infection (days 4, 7, and 10 p.i.; Fig. 7b),
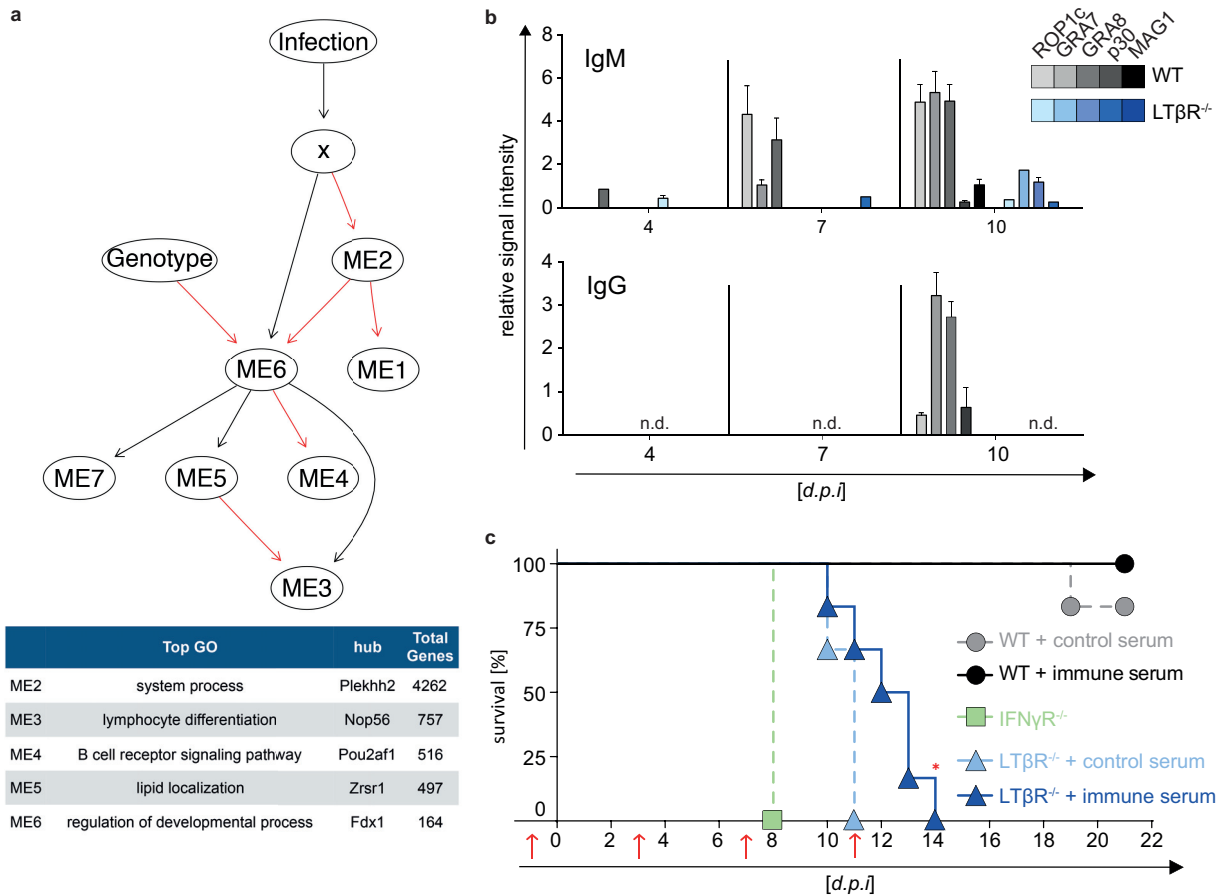
FIG 7 Abrogated parasite-specific isotype class switching and reconstitution of mice with *T. gondii*-specific immune serum. (a) Host-pathogen network prediction model generated based on RNA-seq data of lung tissue of uninfected (d0) and *T. gondii*-infected (ME49, 40 cysts; d7 p.i.) WT and LTβR$^{-/-}$ mice ($n = 3$/group). GmicR was used to detect relationships between module eigengenes (ME) and experimental conditions. X represents the total *T. gondii* gene expression data for each sample; infection and genotype were included as variables. Red lines indicate inverse and black lines positive relationships. Representative gene ontologies and hub genes reported by GmicR for each module are shown in the summary table. (b) *T. gondii*-specific IgM and IgG antibody response in serum of uninfected (d0) and *T. gondii*-infected (ME49, 40 cysts, i.p.) WT and LTβR$^{-/-}$ mice (d4 and d7 p.i., $n = 15$; d10 p.i., $n \geq 20$). Shown is a representative result of four independent experiments; bars represent mean values $\pm$ SEM. (c) Transfer of serum (red arrows; d1, d3, d7, and d11 p.i.) from uninfected donor WT mice (control serum) or from *T. gondii*-infected (ME49, 20 cysts, i.p.) donor WT mice (immune serum) into WT and LTβR$^{-/-}$ acceptor mice. On day 0, acceptor mice ($n = 6$/group) were infected with *T. gondii* (ME49, 10 cysts, i.p.), and survival was evaluated. IFN-γR$^{-/-}$ mice ($n = 3$) served as infection controls. The data shown in panel c represent one experiment. A log rank (Mantel Cox) test was used for the statistical analysis represented in panel c. *, $P < 0.0332$; n.d., not detected.

demonstrating a lack of functional isotype switching that is in line with the bioinformatic host-pathogen prediction network.

LTβR deficiency can be partially compensated for by transfer of *T. gondii* immune serum. Since it has been described that a *T. gondii*-specific IgG response is required for a reduction of the parasite burden (25, 51), we treated LTβR$^{-/-}$ mice with serum from *T. gondii*-infected WT animals (immune serum) and uninfected mice (control serum) and monitored survival after *T. gondii* infection (Fig. 7c). Serum transfer experiments showed that LTβR$^{-/-}$ mice treated with immune serum exhibit significantly prolonged survival (up to day 14 p.i.) compared to littermates that received control serum, which died by day 11 p.i. IFN-γR$^{-/-}$ mice served as infection controls and succumbed as reported around day 8 p.i. (53). These data demonstrate that LTβR-mediated signaling is essential for the development of an efficient humoral immune response to *T. gondii* infection.

DISCUSSION

The results obtained in this study corroborate a profoundly deficient immune response of LTβR$^{-/-}$ mice to *T. gondii* infection and reveal an impaired IFN response, a

severe functional T cell defect, as well as a humoral immune deficiency in the absence of LTβR.

One reason for the significantly increased parasite burden and significantly reduced survival rates of LTβR$^{-/-}$ mice is the inadequate cytokine, especially the IFN-γ, response. The elevated levels of LTα and significantly increased levels of LTβ in the lung of LTβR$^{-/-}$ mice could be caused by compensatory mechanisms and/or lack of negative feedback mechanisms due to the absence of the LTβR. Since we also found elevated levels for IFN-γ, IL-6, IFN-β, IL-1α, and IL-17A and significantly elevated expression levels for IL-1β in the serum and for IL-4 in the lung, we suggest that, overall, uninfected LTβR$^{-/-}$ mice show a dysregulated, more activated, albeit stable immune homeostasis. This is in accordance with the finding that LTβR$^{-/-}$ animals present with splenomegaly, probably due to microbiota-mediated inflammation (54). When *T. gondii* infection disrupts this precarious balance in LTβR$^{-/-}$ mice, the dysregulation becomes more pronounced; on the one hand, LTβR$^{-/-}$ mice have lower levels of IFN-γ in the serum early during infection, but on day 10 p.i., when WT mice already show decreased IFN-γ levels, they remain high in LTβR$^{-/-}$ mice, not only in serum but also in the lungs. Conversely, IL-6 expression in the serum is markedly increased in LTβR$^{-/-}$ mice compared to WT mice throughout the infection. This suggests that by day 10 p.i., parasite expansion is being controlled in WT but not LTβR$^{-/-}$ mice. The significantly increased levels of IL-10 in LTβR mice on day 10 *p.i.* could be a protective/counteractive mechanism to prevent extensive immunopathology (55). Interestingly, several cytokines in LTβR$^{-/-}$ mice are transiently but significantly upregulated on day 4 p.i. This also suggests a disruption of the precarious immune homeostasis in LTβR mice. In contrast to the activated immune homeostasis in LTβR$^{-/-}$ mice, they show decreased expression levels for chemokines/chemokine receptors, genes involved in IFN-γ signaling, and IFN-γ-induced genes in the lung on day 7 p.i. This points toward an inability of LTβR$^{-/-}$ mice to mount an efficient immune response to *T. gondii* infection and is supported by the finding that upregulation of IFN-γ-regulated effector molecules known to be important for *T. gondii* containment, such as iNOS, IDO1, NOX2-gp91phox, and mGBPs, is deficient in LTβR animals. In the lung, in the case of NOX2-gp91phox, this could be due to the lack of TNF-α expression, as it has been shown in *ex vivo* experiments of bronchoalveolar fluid cells and human pulmonary artery endothelial cells that TNF-α upregulates NOX2-g91phox (56, 57). The mRNA expression profile of mGBPs and the protein expression of mGBPs 2 and 7 also fit into this pattern; mGBPs are essential for efficient control of *T. gondii* expansion (31, 33, 58), and RNA-seq analysis shows that uninfected LTβR mice have overall increased expression of, while infected animals show overall less upregulation. And while LTβR$^{-/-}$ animals do upregulate mGBP expression during the course of infection, they show significantly lower expression on day 10 p.i. than WT mice in all cases except for mGBP6/10.

LTβR$^{-/-}$ animals also show increased baseline expression of IFN-γ mRNA in the lung, which would explain the elevated baseline JAK1 protein expression. Increased JAK expression should lead to increased JAK phosphorylation and, consequently, increased STAT1 recruitment and STAT1 phosphorylation (59, 60). However, we observed delayed upregulation of STAT1 and less pSTAT1 protein in infected LTβR$^{-/-}$ animals and therefore hypothesize that the lack of LTβR signaling somehow affects STAT1 expression or recruitment via a so far unknown mechanism. Notably, Kutsch et al. also showed reduced STAT1 expression in LTβR$^{-/-}$ mice (61).

We conclude that, due to the underlying dysregulation of the immune homeostasis, LTβR$^{-/-}$ mice are unable to initiate a coordinated immune response, leading to either delayed upregulation of essential cytokines (e.g., IFN-γ) or overexpression of others (e.g., IL-6, TNF). This is also supported by our findings that LTβR$^{-/-}$ mice do not show the typical splenomegaly associated with (*T. gondii*) infection (39).

In line with published data, we found a virtual absence of NK1.1$^+$ cells in LTβR$^{-/-}$ mice, and NK1.1$^+$ cell numbers dropped in WT mice after infection, probably due to conversion into ILCs (51). Also, a lack of NKT cells has been shown for LTβR$^{-/-}$ mice

(62). Interestingly, a dual role for NKT cells in *T. gondii* infection has been described; on the one hand, they release large amounts of IL-4 and IFN-γ upon activation to shift the T cell response toward a Th1 pattern, and on the other hand, the uncontrolled Th1 response can lead to severe immunopathology (63). Since they have also been indicated in the suppression of a protective immunity against *T. gondii* infection (64), it is maybe not surprising that their numbers are downregulated after infection in WT animals.

Overall, we did not find T cell numbers to be significantly different in either uninfected or *T. gondii*-infected LTβR$^{-/-}$ mice compared to WT mice. However, we found profound defects in T cell effector functions; the reduced number of IFN-γ-producing CD4$^+$ T cells and functional *T. gondii*-specific CD8$^+$ cytotoxic lymphocytes (GzmB$^+$, perforin+, CD107a$^+$) strongly implies that cytotoxic T cell-mediated killing is severely impaired in LTβR$^{-/-}$ animals. Since these responses are known to be essential for efficient *T. gondii* containment, this marked functional deficiency is probably one reason for the susceptibility of LTβR$^{-/-}$ mice to the parasite.

In contrast to T cell numbers, B cell numbers differed significantly in LTβR$^{-/-}$ mice compared to WT mice. On day 10 postinfection, the numbers of CD19$^+$ B cells in WT spleens were significantly lower than those of LTβR$^{-/-}$ animals. This is probably due to maturation of B cells to IgG-producing plasma cells in WT mice, which emigrate to the bone marrow and lose surface CD19 in the process. In LTβR$^{-/-}$ mice, the lack of class switching would inhibit maturation and migration of B cells to the bone marrow.

Since the host-pathogen network prediction model we generated from *T. gondii*-infected mice indicated that the loss of the LTβR inhibits B cell responses, including isotype switching in *T. gondii* infection, we further analyzed the humoral immune response. We demonstrated that *T. gondii*-infected LTβR$^{-/-}$ mice produced less *T. gondii*-specific IgM than WT mice, and no detectable *T. gondii*-specific IgG. Whether this failure is due to impaired IFN-γ production which is an important cytokine for isotype class switching (65) will be determined in the future.

While Glatman Zaretsky et al. (39) argue that the disrupted lymphoid structure, which includes the lack of defined germinal centers in LTβR$^{-/-}$ mice, is the main cause of the reduced antibody response, Ehlers et al. (5) show via bone marrow (BM) chimeras that the effects of LTβR deficiency in *M. tuberculosis* infection cannot be attributed solely to the architectural differences but are also directly caused by the lack of LTβR-mediated signaling. LTα, another member of the TNF/TNFR superfamily, has similar but not identical functions to LTβ in the development of secondary lymphoid organs and immune modulation (2). LTα$^{-/-}$ animals also present with a disturbed architecture of the lymphoid system (no LNs, no PPs, no germinal centers, and a disorganized white pulp) (2, 66). *T. gondii*-infected LTα$^{-/-}$ mice are shown to have reduced numbers of *T. gondii*-specific IFN-γ-producing T cells and lower *T. gondii*-specific antibody titers, but BM chimera experiments demonstrated that an intact secondary lymphoid system is not sufficient to generate an effective immune response (25). Interestingly, the study of Glatman Zaretsky et al. (39), which uses the *T. gondii* Prugniaud strain, also a type II strain, found parasite-specific IgM in serum as early as day 7 postinfection in WT animals, which is in line with our observations in this study. This indicates a comparable timeline in the induction of immune responses and antiparasitic effector mechanisms in WT animals to *T. gondii* in the two type II strains. We therefore feel confident that our results are representative of the infections with a type II strain, which are the prevalent strains in human toxoplasmosis in North America and Europe (67–70).

Although protective B cell responses have been described to play a more significant role in chronic rather than acute *T. gondii* infection in some *T. gondii* infection models (49–51, 71), our data indicate that a robust humoral immune response is dependent on LTβR signaling and is a prerequisite for survival during acute *T. gondii* infection. This conclusion is validated by our data showing that the survival of LTβR$^{-/-}$ animals can be significantly prolonged by transfer of immune serum containing *T. gondii*-specific antibodies.

Finally, the host-pathogen prediction network generated in this study indicates that *T. gondii* infection suppresses B cell responses in WT animals. This could point toward an unknown *T. gondii* strategy to evade the host immune system. Early *T. gondii*-mediated suppression of B cell responses could support dissemination and cyst formation in the brain, facilitating the establishment of chronic infection (25, 72). Since *T. gondii* is known to have developed different mechanisms to evade host immune responses (73), it is worth exploring this approach in the future.

We demonstrate that the loss of LTβR signaling results in a combined and profoundly depressed IFN-γ response, impaired T cell functionality, and the failure to induce parasite-specific IgG antibodies, leading to an increase in parasite burden and fatal outcome of *T. gondii* infection. Therefore, for the first time, we suggest an LTβR-mediated modulation of the IFN-γ signaling pathway *in vivo*. Further understanding of this complex interplay between LTβR and IFN-γ signaling pathways will provide new insights into the pathogenesis of *T. gondii* and may provide novel therapeutic strategies.

MATERIALS AND METHODS

Mice. LTβR$^{-/-}$ mice were previously described (7) and are back-crossed for at least 10 generations onto a C57BL/6N background. Wild-type (WT) littermates were used as controls. Mice were kept under specific-pathogen-free (SPF) conditions in the animal facility at the Heinrich Heine University Düsseldorf and were 8 to 16 weeks old for experiments. Cysts of the ME49 strain (substrain 2017) of *T. gondii* were collected from the brain tissue of chronically infected CD1 mice. All animal experiments were conducted in strict accordance with the German Animal Welfare Act. The protocols were approved by the local authorities (Permit no. 84-02.04.2013.A495, 81-02.04.2018.A406, and 81-02.05.40.18.082). All applicable international, national, and institutional guidelines for the care and use of animals were followed.

***Toxoplasma gondii* infection experiments.** Mice were intraperitoneally (i.p.) infected with 40 cysts (ME49 strain) and weighed and scored daily for the duration of the experiments. Mice were euthanized on days 4, 7, and 10 postinfection (dpi); uninfected mice (d0) served as controls. After euthanasia (100 mg/kg ketamine, 10 mg/kg xylazine; Vétoquinol GmbH), blood was taken from the vena cava inferior, and spleen, lung, and muscle tissue was harvested for analysis.

Detection of parasite load. Total DNA was isolated from tissues using a DNA isolation kit (Genekam) according to the manufacturer's protocol. qRT-PCR was performed on a Bio-Rad CFX-96 Touch real-time detection system. To determine parasite load, PCR of DNA isolated from defined numbers (101 to 105) of *in vitro*-cultured ME49 tachyzoites (using distilled water [dH$_2$O] as a negative control) was performed to generate a standard curve; TgB1 primers and probe (Metabion) were used to amplify a defined sequence of the 35-fold repetitive B1 gene from *T. gondii* and are listed in Table S1. This *T. gondii* standard curve was used to determine B1 amplification for calculation of parasite load.

Cytokine measurement. Cytokines CCL2, IFN-γ, IFN-β, IL-1α, IL-1β, IL-6, IL-10, IL12p70, IL-17A, IL-23, IL-27, and TNF-α were measured using the LEGENDplex mouse inflammation panel (BioLegend) according to the manufacturer's protocol. Samples were measured using a BD FACSCanto II instrument.

Real-time qRT-PCR. Total RNA was isolated from tissues using the TRIzol reagent (Invitrogen) according to the manufacturer's protocol. cDNA was reverse-transcribed using SuperScript III reverse transcriptase (200 U/μl; Invitrogen). qRT-PCR was performed on the Bio-Rad CFX-96 Touch real-time detection system. The primer sequences and corresponding probes (Metabion, Roche, and TIB Molbiol) are listed in Table S1. Results are expressed relative to expression in untreated WT mice normalized to β-actin ($2^{-\Delta\Delta CT}$).

RNA-seq analysis. Lung tissue of uninfected (d0) and *T. gondii*-infected (ME49 strain, 40 cysts, i.p.) WT and LTβR$^{-/-}$ mice was obtained, and RNA sequencing was performed on a HiSeq 3000 device. Mouse and *T. gondii* transcripts were quantified from FASTQ files using Salmon with default settings and GC bias compensation. For transcriptome models, *Mus musculus* GRCm38 cDNA (ensembl.org, release-97) and *Tgondii*ME49 annotated transcripts (toxodb.org, ToxoDB-45) were used. Mouse transcripts from pseudogenes or with retained introns were excluded prior to conversion to gene counts using the DESeq2 package. Non-protein-encoding *T. gondii* transcripts were excluded prior to conversion to gene counts. DEseq2 was used to test for genotype-specific responsiveness to infection with the following model: ~genotype · infection. To calculate WT-specific responsiveness, we used the following model: ~genotype + genotype: infection. For significance, the Wald test with an adjusted *P* value of 0.1 was used.

Host-pathogen network generation. Previously developed analytic tools for 'omics data sets were used to generate the host-pathogen network as described (74). Prior to network generation, the variance stabilizing transformation (VST)-normalized data were filtered for genes that showed significant differential expression for at least one contrast. This produced an expression matrix for 10,748 genes. The GmicR package was then used for module detection, using a minimum module size of 30, mergeCutHeight of 0.3, and Rsquared cut of 0.80. To detect relationships between modules and infection, VST-normalized data *T. gondii* expression levels for each sample were aggregated by sum, and then these numeric data were merged to module eigengenes using the Data_Prep function of GmicR (Fig. S6). Genotype and infection conditions were merged with the discretized data. A white list

indicating the parent-to-child relationship from "genotype" to "ME6" corresponding to the module containing LTβR was included in the Bayesian network learning process. A final network was generated using the bn_tabu_gen function with 500 bootstrap replicates, "bds" score, and iss set to 1. Inverse relationships between nodes were detected using the InverseARCs function from GmicR with default settings.

Immunoblot analysis and antibodies. Tissues were homogenized in phosphate-buffered saline (PBS) containing cOmplete protease inhibitor cocktail (Roche) using the Precellys homogenizer (Bertin). The protein concentration was measured using the Pierce BCA protein assay kit (Thermo Scientific) according to the manufacturer's protocol. Samples ($10\,\mu$g/lane) were separated by 4 to 12% SDS-PAGE, followed by electrophoretic transfer to nitrocellulose membranes before blocking and incubation with the primary antibodies listed in Table S2. Horseradish peroxidase (HRP)-labeled anti-rabbit or anti-mouse antibodies (Cell Signaling Technologies) were used as secondary antibodies. Relative signal intensity of protein bands was quantified using ImageJ (NIH).

tSNE. The cloud-based platform Cytobank (75) (Mountain View) was used for visualization of flow cytometry data. A total of 60,000 events per sample were analyzed (parameters: iterations, 2,400; perplexity, 80; Theta, 0.5) before overlaid dot plots were generated.

Flow cytometry. Spleens were harvested and digested for 30 min at 37°C using collagenase D (100 mg/ml) and DNase I (20,000 U/ml). Tissue digest was stopped using $1\times$ PBS containing 10 mM EDTA before cell solution was filtered using a 70-μm cell strainer. A red blood cell (RBC) lysis (Merck) was performed before cell numbers were calculated. Single-cell suspended splenocytes (1×10^6 cells) were stained with the fixable viability dye eFluor 780 (eBioscience). Surface staining with antibodies specific for CD3e (145-2c11), CD4 (RM4-5), CD8a (53-6.7), CD19 (6D5), CD25 (3C7), and NK1.1 (PK136), all purchased from BioLegend (expect for CD4, which as purchased from BD Bioscience), was performed. For intracellular staining, splenocytes were incubated for 20 h with toxoplasma lysate antigen (TLA, $15\,\mu$g/ml) before brefeldin A (eBioscience) was added for an additional 4 h. After surface staining with anti-CD4 (RM4-5), anti-CD8a (53-6.7), anti-CD107a (1D4B), and anti-TCRb (H57-597), cells were fixed, permeabilized, and stained with anti-IFN-γ (XMG1.2), anti-granzyme B (QA16A02), and antiperforin (S16009A) (all purchased from BioLegend) using a Fix & Perm cell permeabilization kit (Life Technologies) according to the manufacturer's protocol. Major histocompatibility complex class I-SVLAFRRL pentamer was purchased from ProImmune and used in experiments as indicated. BD Calibrate beads (BD Bioscience) were added to the samples before acquisition with a BD LSRFortessa instrument.

Detection of *T. gondii*-specific antibodies. A RecomLine *Toxoplasma* IgG/IgM kit (Mikrogen Diagnostik) was used to detect IgM and IgG antibodies against *T. gondii* in serum. Anti-human IgM and IgG conjugates provided within the kit were replaced with anti-mouse IgM-HRP-labeled (Invitrogen) and anti-mouse IgG-HRP-labeled (Invitrogen) conjugates. Otherwise, the assay was performed according to the manufacturer's protocol.

Serum transfer. Blood from naive donor mice (control serum) or WT mice infected i.p. with 20 cysts of the ME49 strain of *T. gondii* (immune serum) was collected from the vena cava inferior. After 2 h of incubation at room temperature (RT), serum was collected by centrifugation of the blood. Acceptor WT and LTβR$^{-/-}$ mice were reconstituted intraperitoneally with 0.2 ml serum 1 day prior to infection (d-1) as well as on days 3, 7, and 11 p.i. Acceptor (WT and LTβR$^{-/-}$) mice as well as IFN-γ$^{-/-}$ control mice were intraperitoneally infected with 10 cysts (ME49 strain) and weighed and scored daily for the duration of the experiment. *T. gondii*-specific antibodies were detected via line blots to confirm the presence and assess the amount of *T. gondii*-specific antibodies in control and immune serum.

Statistical analysis. Data were analyzed with Prism version 8 (GraphPad) using a log rank (Mantel Cox) test or 2-way analysis of variance (ANOVA) corrected for multiple comparison by the Tukey's or Sidak's *post hoc* test as indicated in the figure legends. Symbols represent individual animals, columns represent mean values, and error bars represent the $\pm$ standard error of the mean (SEM). *P* values of $\leq$0.0332 were considered statistically significant and marked with asterisks. *P* values of $\geq$0.0332 were considered statistically not significant and were not specifically marked.

Data availability. The data that support the findings of this study are available from the corresponding author.

SUPPLEMENTAL MATERIAL

Supplemental material is available online only.
SUPPLEMENTAL FILE 1, PDF file, 6.3 MB.

ACKNOWLEDGMENTS

REFERENCES

1. Ward-Kavanagh LK, Lin WW, Sedy JR, Ware CF. 2016. The TNF receptor superfamily in co-stimulating and co-inhibitory responses. Immunity 44:1005–1019. https://doi.org/10.1016/j.immuni.2016.04.019.

2. Hehlgans T, Pfeffer K. 2005. The intriguing biology of the tumour necrosis factor/tumour necrosis factor receptor superfamily: players, rules and the games. Immunology 115:1–20. https://doi.org/10.1111/j.1365-2567.2005.02143.x.

3. Schneider K, Potter KG, Ware CF. 2004. Lymphotoxin and LIGHT signaling pathways and target genes. Immunol Rev 202:49–66. https://doi.org/10.1111/j.0105-2896.2004.00206.x.

4. Ware CF. 2005. Network communications: lymphotoxins, LIGHT, and TNF. Annu Rev Immunol 23:787–819. https://doi.org/10.1146/annurev.immunol.23.021704.115719.

5. Ehlers S, Holscher C, Scheu S, Tertilt C, Hehlgans T, Suwinski J, Endres R, Pfeffer K. 2003. The lymphotoxin beta receptor is critically involved in controlling infections with the intracellular pathogens Mycobacterium tuberculosis and Listeria monocytogenes. J Immunol 170:5210–5218. https://doi.org/10.4049/jimmunol.170.10.5210.

6. Spahn TW, Maaser C, Eckmann L, Heidemann J, Lugering A, Newberry R, Domschke W, Herbst H, Kucharzik T. 2004. The lymphotoxin-beta receptor is critical for control of murine Citrobacter rodentium-induced colitis. Gastroenterology 127:1463–1473. https://doi.org/10.1053/j.gastro.2004.08.022.

7. Futterer A, Mink K, Luz A, Kosco-Vilbois MH, Pfeffer K. 1998. The lymphotoxin beta receptor controls organogenesis and affinity maturation in peripheral lymphoid tissues. Immunity 9:59–70. https://doi.org/10.1016/s1074-7613(00)80588-9.

8. Wu Q, Sun Y, Wang J, Lin X, Wang Y, Pegg LE, Futterer A, Pfeffer K, Fu YX. 2001. Signal via lymphotoxin-beta R on bone marrow stromal cells is required for an early checkpoint of NK cell development. J Immunol 166:1684–1689. https://doi.org/10.4049/jimmunol.166.3.1684.

9. Banks TA, Rickert S, Ware CF. 2006. Restoring immune defenses via lymphotoxin signaling: lessons from cytomegalovirus. Immunol Res 34:243–254. https://doi.org/10.1385/IR:34:3:243.

10. Puglielli MT, Browning JL, Brewer AW, Schreiber RD, Shieh WJ, Altman JD, Oldstone MB, Zaki SR, Ahmed R. 1999. Reversal of virus-induced systemic shock and respiratory failure by blockade of the lymphotoxin pathway. Nat Med 5:1370–1374. https://doi.org/10.1038/70938.

11. Jin L, Guo X, Shen C, Hao X, Sun P, Li P, Xu T, Hu C, Rose O, Zhou H, Yang M, Qin CF, Guo J, Peng H, Zhu M, Cheng G, Qi X, Lai R. 2018. Salivary factor LTRIN from Aedes aegypti facilitates the transmission of Zika virus by interfering with the lymphotoxin-beta receptor. Nat Immunol 19:342–353. https://doi.org/10.1038/s41590-018-0063-9.

12. Behnke K, Sorg UR, Gabbert HE, Pfeffer K. 2017. The lymphotoxin beta receptor is essential for upregulation of IFN-induced guanylate-binding proteins and survival after Toxoplasma gondii infection. Mediators Inflamm 2017:7375818. https://doi.org/10.1155/2017/7375818.

13. Hill DE, Chirukandoth S, Dubey JP. 2005. Biology and epidemiology of Toxoplasma gondii in man and animals. Anim Health Res Rev 6:41–61. https://doi.org/10.1079/ahr2005100.

14. Saadatnia G, Golkar M. 2012. A review on human toxoplasmosis. Scand J Infect Dis 44:805–814. https://doi.org/10.3109/00365548.2012.693197.

15. Montoya JG, Liesenfeld O. 2004. Toxoplasmosis. Lancet 363:1965–1976. https://doi.org/10.1016/S0140-6736(04)16412-X.

16. Hakimi MA, Olias P, Sibley LD. 2017. Toxoplasma effectors targeting host signaling and transcription. Clin Microbiol Rev 30:615–645. https://doi.org/10.1128/CMR.00005-17.

17. Petersen E. 2007. Toxoplasmosis. Semin Fetal Neonatal Med 12:214–223. https://doi.org/10.1016/j.siny.2007.01.011.

18. Gaddi PJ, Yap GS. 2007. Cytokine regulation of immunopathology in toxoplasmosis. Immunol Cell Biol 85:155–159. https://doi.org/10.1038/sj.icb.7100038.

19. Denkers EY. 1999. T lymphocyte-dependent effector mechanisms of immunity to Toxoplasma gondii. Microbes Infect 1:699–708. https://doi.org/10.1016/S1286-4579(99)80071-9.

20. Ivanova DL, Denton SL, Fettel KD, Sondgeroth KS, Munoz Gutierrez J, Bangoura B, Dunay IR, Gigley JP. 2019. Innate lymphoid cells in protection, pathology, and adaptive immunity during apicomplexan infection. Front Immunol 10:196. https://doi.org/10.3389/fimmu.2019.00196.

21. Darwich L, Coma G, Pena R, Bellido R, Blanco EJ, Este JA, Borras FE, Clotet B, Ruiz L, Rosell A, Andreo F, Parkhouse RM, Bofill M. 2009. Secretion of interferon-gamma by human macrophages demonstrated at the single-cell level after costimulation with interleukin (IL)-12 plus IL-18. Immunology 126:386–393. https://doi.org/10.1111/j.1365-2567.2008.02905.x.

22. Suzuki Y, Orellana MA, Schreiber RD, Remington JS. 1988. Interferon-gamma: the major mediator of resistance against Toxoplasma gondii. Science 240:516–518. https://doi.org/10.1126/science.3128869.

23. Yap GS, Sher A. 1999. Cell-mediated immunity to Toxoplasma gondii: initiation, regulation and effector function. Immunobiology 201:240–247. https://doi.org/10.1016/S0171-2985(99)80064-3.

24. Saeij JP, Frickel EM. 2017. Exposing Toxoplasma gondii hiding inside the vacuole: a role for GBPs, autophagy and host cell death. Curr Opin Microbiol 40:72–80. https://doi.org/10.1016/j.mib.2017.10.021.

25. Schluter D, Kwok LY, Lutjen S, Soltek S, Hoffmann S, Korner H, Deckert M. 2003. Both lymphotoxin-alpha and TNF are crucial for control of Toxoplasma gondii in the central nervous system. J Immunol 170:6172–6182. https://doi.org/10.4049/jimmunol.170.12.6172.

26. Daubener W, Remscheid C, Nockemann S, Pilz K, Seghrouchni S, Mackenzie C, Hadding U. 1996. Anti-parasitic effector mechanisms in human brain tumor cells: role of interferon-gamma and tumor necrosis factor-alpha. Eur J Immunol 26:487–492. https://doi.org/10.1002/eji.1830260231.

27. Fox BA, Gigley JP, Bzik DJ. 2004. Toxoplasma gondii lacks the enzymes required for de novo arginine biosynthesis and arginine starvation triggers cyst formation. Int J Parasitol 34:323–331. https://doi.org/10.1016/j.ijpara.2003.12.001.

28. Pfefferkorn ER, Rebhun S, Eckel M. 1986. Characterization of an indoleamine 2,3-dioxygenase induced by gamma-interferon in cultured human fibroblasts. J Interferon Res 6:267–279. https://doi.org/10.1089/jir.1986.6.267.

29. Scharton-Kersten TM, Yap G, Magram J, Sher A. 1997. Inducible nitric oxide is essential for host control of persistent but not acute infection with the intracellular pathogen Toxoplasma gondii. J Exp Med 185:1261–1273. https://doi.org/10.1084/jem.185.7.1261.

30. Degrandi D, Konermann C, Beuter-Gunia C, Kresse A, Wurthner J, Kurig S, Beer S, Pfeffer K. 2007. Extensive characterization of IFN-induced GTPases mGBP1 to mGBP10 involved in host defense. J Immunol 179:7729–7740. https://doi.org/10.4049/jimmunol.179.11.7729.

31. Steffens N, Beuter-Gunia C, Kravets E, Reich A, Legewie L, Pfeffer K, Degrandi D. 2020. Essential role of mGBP7 for survival of Toxoplasma gondii infection. mBio 11:e02993-19.https://doi.org/10.1128/mBio.02993-19.

32. Yamamoto M, Okuyama M, Ma JS, Kimura T, Kamiyama N, Saiga H, Ohshima J, Sasai M, Kayama H, Okamoto T, Huang DC, Soldati-Favre D, Horie K, Takeda J, Takeda K. 2012. A cluster of interferon-gamma-inducible p65 GTPases plays a critical role in host defense against Toxoplasma gondii. Immunity 37:302–313. https://doi.org/10.1016/j.immuni.2012.06.009.

33. Degrandi D, Kravets E, Konermann C, Beuter-Gunia C, Klumpers V, Lahme S, Wischmann E, Mausberg AK, Beer-Hammer S, Pfeffer K. 2013. Murine guanylate binding protein 2 (mGBP2) controls Toxoplasma gondii replication. Proc Natl Acad Sci U S A 110:294–299. https://doi.org/10.1073/pnas.1205635110.

34. Clough B, Frickel EM. 2017. The toxoplasma parasitophorous vacuole: an evolving host-parasite frontier. Trends Parasitol 33:473–488. https://doi.org/10.1016/j.pt.2017.02.007.

35. Selleck EM, Fentress SJ, Beatty WL, Degrandi D, Pfeffer K, Virgin HW, IV, Macmicking JD, Sibley LD. 2013. Guanylate-binding protein 1 (Gbp1) contributes to cell-autonomous immunity against Toxoplasma gondii. PLoS Pathog 9:e1003320. https://doi.org/10.1371/journal.ppat.1003320.

36. Kravets E, Degrandi D, Ma Q, Peulen TO, Klumpers V, Felekyan S, Kuhnemuth R, Weidtkamp-Peters S, Seidel CA, Pfeffer K. 2016. Guanylate binding proteins directly attack Toxoplasma gondii via supramolecular complexes. Elife 5:e11479. https://doi.org/10.7554/eLife.11479.

37. Yap GS, Scharton-Kersten T, Charest H, Sher A. 1998. Decreased resistance of TNF receptor p55- and p75-deficient mice to chronic toxoplasmosis despite normal activation of inducible nitric oxide synthase in vivo. J Immunology 160:1340–1345.

38. Deckert-Schluter M, Bluethmann H, Rang A, Hof H, Schluter D. 1998. Crucial role of TNF receptor type 1 (p55), but not of TNF receptor type 2 (p75), in murine toxoplasmosis. J Immunol 160:3427–3436.

39. Glatman Zaretsky A, Silver JS, Siwicki M, Durham A, Ware CF, Hunter CA. 2012. Infection with Toxoplasma gondii alters lymphotoxin expression associated with changes in splenic architecture. Infect Immun 80:3602–3610. https://doi.org/10.1128/IAI.00333-12.

40. Gazzinelli RT, Eltoum I, Wynn TA, Sher A. 1993. Acute cerebral toxoplasmosis is induced by in vivo neutralization of TNF-alpha and correlates with the down-regulated expression of inducible nitric oxide synthase and other markers of macrophage activation. J Immunol 151:3672–3681.

41. Schaper F, Rose-John S. 2015. Interleukin-6: biology, signaling and strategies of blockade. Cytokine Growth Factor Rev 26:475–487. https://doi.org/10.1016/j.cytogfr.2015.07.004.

42. Saraiva M, O'Garra A. 2010. The regulation of IL-10 production by immune cells. Nat Rev Immunol 10:170–181. https://doi.org/10.1038/nri2711.

43. Brenier-Pinchart MP, Villena I, Mercier C, Durand F, Simon J, Cesbron-Delauw MF, Pelloux H. 2006. The Toxoplasma surface protein SAG1 triggers efficient in vitro secretion of chemokine ligand 2 (CCL2) from human fibroblasts. Microbes Infect 8:254–261. https://doi.org/10.1016/j.micinf.2005.06.023.

44. Singhania A, Graham CM, Gabrysova L, Moreira-Teixeira L, Stavropoulos E, Pitt JM, Chakravarty P, Warnatsch A, Branchett WJ, Conejero L, Lin JW, Davidson S, Wilson MS, Bancroft G, Langhorne J, Frickel E, Sesay AK, Priestnall SL, Herbert E, Ioannou M, Wang Q, Humphreys IR, Dodd J, Openshaw PJM, Mayer-Barber KD, Jankovic D, Sher A, Lloyd CM, Baldwin N, Chaussabel D, Papayannopoulos V, Wack A, Banchereau JF, Pascual VM, O'Garra A. 2019. Transcriptional profiling unveils type I and II interferon networks in blood and tissues across diseases. Nat Commun 10:2887. https://doi.org/10.1038/s41467-019-10601-6.

45. Yarovinsky F. 2014. Innate immunity to Toxoplasma gondii infection. Nat Rev Immunol 14:109–121. https://doi.org/10.1038/nri3598.

46. Ratna A, Arora SK. 2016. Leishmania recombinant antigen modulates macrophage effector function facilitating early clearance of intracellular parasites. Trans R Soc Trop Med Hyg 110:610–619. https://doi.org/10.1093/trstmh/trw068.

47. Koo SJ, Chowdhury IH, Szczesny B, Wan X, Garg NJ. 2016. Macrophages promote oxidative metabolism to drive nitric oxide generation in response to Trypanosoma cruzi. Infect Immun 84:3527–3541. https://doi.org/10.1128/IAI.00809-16.

48. Ufermann CM, Domrose A, Babel T, Tersteegen A, Cengiz SC, Eller SK, Spekker-Bosker K, Sorg UR, Forster I, Daubener W. 2019. Indoleamine 2,3-dioxygenase activity during acute toxoplasmosis and the suppressed T cell proliferation in mice. Front Cell Infect Microbiol 9:184. https://doi.org/10.3389/fcimb.2019.00184.

49. Pittman KJ, Knoll LJ. 2015. Long-Term Relationships: the Complicated Interplay between the Host and the Developmental Stages of Toxoplasma gondii during Acute and Chronic Infections. Microbiol Mol Biol Rev 79:387–401. https://doi.org/10.1128/MMBR.00027-15.

50. Sher A, Denkers EY, Gazzinelli RT. 1995. Induction and regulation of host cell-mediated immunity by Toxoplasma gondii. Ciba Found Symp 195:95–104. discussion 104–9. https://doi.org/10.1002/9780470514849.ch7.

51. Park E, Patel S, Wang Q, Andhey P, Zaitsev K, Porter S, Hershey M, Bern M, Plougastel-Douglas B, Collins P, Colonna M, Murphy KM, Oltz E, Artyomov M, Sibley LD, Yokoyama WM. 2019. Toxoplasma gondii infection drives conversion of NK cells into ILC1-like cells. Elife 8:95. https://doi.org/10.7554/eLife.47605.

52. Vallabhapurapu S, Powolny-Budnicka I, Riemann M, Schmid RM, Paxian S, Pfeffer K, Korner H, Weih F. 2008. Rel/NF-kappaB family member RelA regulates NK1.1- to NK1.1+ transition as well as IL-15-induced expansion of NKT cells. Eur J Immunol 38:3508–3519. https://doi.org/10.1002/eji.200737830.

53. Deckert-Schluter M, Rang A, Weiner D, Huang S, Wiestler OD, Hof H, Schluter D. 1996. Interferon-gamma receptor-deficiency renders mice highly susceptible to toxoplasmosis by decreased macrophage activation. Lab Invest 75:827–841.

54. Zhang Y, Kim TJ, Wroblewska JA, Tesic V, Upadhyay V, Weichselbaum RR, Tumanov AV, Tang H, Guo X, Tang H, Fu YX. 2018. Type 3 innate lymphoid cell-derived lymphotoxin prevents microbiota-dependent inflammation. Cell Mol Immunol 15:697–709. https://doi.org/10.1038/cmi.2017.25.

55. Gazzinelli RT, Wysocka M, Hieny S, Scharton-Kersten T, Cheever A, Kuhn R, Muller W, Trinchieri G, Sher A. 1996. In the absence of endogenous IL-10, mice acutely infected with Toxoplasma gondii succumb to a lethal immune response dependent on CD4+ T cells and accompanied by overproduction of IL-12, IFN-gamma and TNF-alpha. J Immunol 157:798–805.

56. Frey RS, Rahman A, Kefer JC, Minshall RD, Malik AB. 2002. PKCzeta regulates TNF-alpha-induced activation of NADPH oxidase in endothelial cells. Circ Res 90:1012–1019. https://doi.org/10.1161/01.res.0000017631.28815.8e.

57. Ziltener P, Reinheckel T, Oxenius A. 2016. Neutrophil and alveolar macrophage-mediated innate immune control of Legionella pneumophila lung infection via TNF and ROS. PLoS Pathog 12:e1005591. https://doi.org/10.1371/journal.ppat.1005591.

58. Ohshima J, Lee Y, Sasai M, Saitoh T, Su Ma J, Kamiyama N, Matsuura Y, Pann-Ghill S, Hayashi M, Ebisu S, Takeda K, Akira S, Yamamoto M. 2014. Role of mouse and human autophagy proteins in IFN-gamma-induced cell-autonomous responses against Toxoplasma gondii. J Immunol 192:3328–3335. https://doi.org/10.4049/jimmunol.1302822.

59. Kisseleva T, Bhattacharya S, Braunstein J, Schindler CW. 2002. Signaling through the JAK/STAT pathway, recent advances and future challenges. Gene 285:1–24. https://doi.org/10.1016/s0378-1119(02)00398-0.

60. Greenlund AC, Farrar MA, Viviano BL, Schreiber RD. 1994. Ligand-induced IFN gamma receptor tyrosine phosphorylation couples the receptor to its signal transduction system (p91). EMBO J 13:1591–1600. https://doi.org/10.1002/j.1460-2075.1994.tb06422.x.

61. Kutsch S, Degrandi D, Pfeffer K. 2008. Immediate lymphotoxin beta receptor-mediated transcriptional response in host defense against L. monocytogenes. Immunobiology 213:353–366. https://doi.org/10.1016/j.imbio.2007.10.011.

62. Franki AS, Van Beneden K, Dewint P, Hammond KJ, Lambrecht S, Leclercq G, Kronenberg M, Deforce D, Elewaut D. 2006. A unique lymphotoxin {alpha}beta-dependent pathway regulates thymic emigration of V{alpha}14 invariant natural killer T cells. Proc Natl Acad Sci U S A 103:9160–9165. https://doi.org/10.1073/pnas.0508892103.

63. Ronet C, Darche S, Leite de Moraes M, Miyake S, Yamamura T, Louis JA, Kasper LH, Buzoni-Gatel D. 2005. NKT cells are critical for the initiation of an inflammatory bowel response against Toxoplasma gondii. J Immunol 175:899–908. https://doi.org/10.4049/jimmunol.175.2.899.

64. Nakano Y, Hisaeda H, Sakai T, Ishikawa H, Zhang M, Maekawa Y, Zhang T, Takashima M, Nishitani M, Good RA, Himeno K. 2002. Roles of NKT cells in resistance against infection with Toxoplasma gondii and in expression of heat shock protein 65 in the host macrophages. Microbes Infect 4:1–11. https://doi.org/10.1016/s1286-4579(01)01503-9.

65. Paludan SR. 1998. Interleukin-4 and interferon-gamma: the quintessence of a mutual antagonistic relationship. Scand J Immunol 48:459–468. https://doi.org/10.1046/j.1365-3083.1998.00435.x.

66. De Togni P, Goellner J, Ruddle NH, Streeter PR, Fick A, Mariathasan S, Smith SC, Carlson R, Shornick LP, Strauss-Schoenberger J. 1994. Abnormal development of peripheral lymphoid organs in mice deficient in lymphotoxin. Science 264:703–707. https://doi.org/10.1126/science.8171322.

67. Sibley LD, Boothroyd JC. 1992. Virulent strains of Toxoplasma gondii comprise a single clonal lineage. Nature 359:82–85. https://doi.org/10.1038/359082a0.

68. Howe DK, Sibley LD. 1995. Toxoplasma gondii comprises three clonal lineages: correlation of parasite genotype with human disease. J Infect Dis 172:1561–1566. https://doi.org/10.1093/infdis/172.6.1561.

69. Howe DK, Honore S, Derouin F, Sibley LD. 1997. Determination of genotypes of Toxoplasma gondii strains isolated from patients with toxoplasmosis. J Clin Microbiol 35:1411–1414. https://doi.org/10.1128/JCM.35.6.1411-1414.1997.

70. Schlüter D, Däubener W, Schares G, Groß U, Pleyer U, Lüder C. 2014. Animals are key to human toxoplasmosis. Int J Med Microbiol 304:917–929. https://doi.org/10.1016/j.ijmm.2014.09.002.

71. Kang H, Remington JS, Suzuki Y. 2000. Decreased resistance of B cell-deficient mice to infection with Toxoplasma gondii despite unimpaired expression of IFN-gamma, TNF-alpha, and inducible nitric oxide synthase. J Immunol 164:2629–2634. https://doi.org/10.4049/jimmunol.164.5.2629.

72. Schluter D, Deckert M, Hof H, Frei K. 2001. Toxoplasma gondii infection of neurons induces neuronal cytokine and chemokine production, but gamma interferon- and tumor necrosis factor-stimulated neurons fail to inhibit the invasion and growth of T. gondii. Infect Immun 69:7889–7893. https://doi.org/10.1128/IAI.69.12.7889-7893.2001.

73. Zhu W, Li J, Pappoe F, Shen J, Yu L. 2019. Strategies developed by Toxoplasma gondii to survive in the host. Front Microbiol 10:899. https://doi.org/10.3389/fmicb.2019.00899.

74. Virgen-Slane R, Correa RG, Ramezani-Rad P, Steen-Fuentes S, Detanico T, DiCandido MJ, Li J, Ware CF. 2020. Cutting edge: the RNA-binding protein Ewing sarcoma is a novel modulator of lymphotoxin beta receptor signaling. J Immunol 204:1085–1090. https://doi.org/10.4049/jimmunol.1901260.

75. Chen TJ, Kotecha N. 2014. Cytobank: providing an analytics platform for community cytometry data analysis and collaboration. Curr Top Microbiol Immunol 377:127–157. https://doi.org/10.1007/82_2014_364.